공학박사 학위논문

Biomolecule Immobilization Platforms Based on Pentafluorophenyl Acrylate Polymers

펜타플루오로페닐 아크릴레이트 고분자를 기반으로 한 생체분자 고정용 플랫폼의 제조

2018년 8 월

서울대학교 대학원

화학생물공학부

손 현 주

Abstract

Biomolecule Immobilization Platforms Based on Pentafluorophenyl Acrylate Polymers

Hyunjoo Son

School of Chemical & Biological Engineering

The Graduate School

Seoul National University

Functional polymers have had attention and been expected as a promising materials in a wide range of application fields such as biotechnology, photonics, and optoelectronics, and biocompatibility. The physical or chemical properties and nanostructures constituted of functional polymer should be controlled by diverse synthesis and processing methods. As more complicated platforms based on functional polymers required, reactive ester polymers were utilized for both preparation of novel polymeric precursors and for the fabrication of reactive polymer-

based platforms with desired functionalities and forms. The controlled radical polymerization techniques were utilized to yield in well-defined polymers and polymer-based films and brushes. Furthermore, modification of reactive polymer platforms results in facile approaches to bio-applications by covalent immobilization of biomolecules. In this thesis, poly(pentafluorophenyl acrylate) (poly(PFPA)), one of active ester polymers, was realized in the structures of thin films and polymer brushes and considered as biomolecule immobilization platforms through post-polymerization modification methods using its high reactivity with amines. The brief introduce about reactive polymer and synthesis methods and biomolecule immobilization are in chapter 1.

In chapter 2, we investigate the mechanism in primary amine-induced post-polymerization modification of spin-cast active ester polymer thin films, comprised of poly(PFPA). The most important physical parameters in the post-modification are the molecular weight of PFPA polymers and the aliphatic chain length of primary amines. The effect of two parameters on the penetration depth as well as the exchange kinetics was systematically studied by neutron reflectivity (NR) and quartz crystal microbalance (QCM-D), accompanied by the surface morphological changes measured by an atomic force microscope (AFM) and an optical microscope (OM). The spin-cast thin films of high and low molecular weight of poly(PFPA) showed the distinctive difference originating from the primary alkyl amines of different alkyl chain length. The aliphatic chain length of primary alkyl amines dramatically influenced the penetration kinetics into low molecular weight poly(PFPA) films

whereas there was no significant penetration effect on the high molecular weight films. The high molecular weight of poly(PFPA) films led to the deceleration of dissolution of amine-functionalized polymer chains in good solvent. Both alkyl chain length of primary alkyl amines and the molecular weight of poly(PFPA) affect the penetration depth and dissolution of the polymer chains from the surface of thin films, respectively.

In chapter 3, we present the synthesis of reactive polymer brushes prepared by surface-initiated (SI) RAFT polymerization of pentafluorophenyl acrylate. Dithiobenzoic acid benzyl-(4-ethyltrimethoxylsilyl) ester was used as the surface-initiated RAFT chain transfer agent (SI-CTA) and the anchoring group onto the silica particles. Poly(pentafluorophenyl acrylate) (poly(PFPA)) is known to have high and selective reactivity with amine functional groups that offers facile routes to realize diverse functions starting from the same platforms by simple post-polymerization modification with amines. Through the grafting-from approach, polymer brushes with controlled molecular weight and conformal coverage were obtained. The synthesis and utilization of reactive polymer brushes offers an easy approach in the controlled-fabrication of polymer brushes with desired functionality, which is limited by other strategies.

In chapter 4, we reported the poly(PFPA) brush-based platforms for antibody-antigen precipitation or immunoprecipitation (IP), which are routinely performed by biologists to isolate specific antigens and to identify their interactors from complex protein mixtures. The conventional approach involving agarose supports shows reasonably good antibody-binding capability due to their selective bioaffinity

immobilization, but often suffers from high nonspecific binding and antibody contamination. We prepared silica particles containing poly(PFPA) brushes, prepared by the reversible addition-fragmentation chain transfer (SI-RAFT) polymerization. Upon sequential functionalization with antibodies and polyethylene glycol (PEG), it showed significantly reduced nonspecific protein adsorption and complete elimination of antibody contamination. Furthermore, by optimizing the two parameters such as molecular weight of the polymer brushes and the amount of PEG passivates, the poly(PFPA) brush-grafted particles show the highest efficiency. Taking into account their versatility and convenient features of such reactive brush platforms, the poly(PFPA) platforms have the potential to be an alternative to traditional agarose-based platforms for immunoprecipitation.

In chapter 5, we briefly introduced about poly(PFPA)-coated channel for the application of biosensors. Substrates which have amine functional groups on the surface were coated with poly(PFPA) as loop or train configuration of grafted brushes. To get more stability of poly(PFPA) films during incubation process in antibody solution, many conditions were tested and characterized by confocal images. Some functional groups in poly(PFPA) chains reacted with amine groups on substrates and the other remained groups were used for immobilization of fluorescent antibodies. Based on the fabrication of channel on the poly(PFPA)-coated substrates, we expected this simply fabricated poly(PFPA)-based platforms can be applied as biosensor for primary diagnosis.

In conclusion, reactive poly(PFPA) platforms that allow facile preparation of

functional material was demonstrated from polymer films to polymer brush particles. The reactive poly(PFPA) thin films and particles based on the simple and quantitative post-modification with amine-containing molecules could be utilized for many practical applications due to the ease of control over the degree of functionalization. Our system and the strategy would provide a facile process towards functional polymer film, and polymer brushes by eliminating difficult multistep of synthesis. Furthermore, the possibility of poly(PFPA)-based platforms for the use in bioapplications such as purification and biosensing was confirmed.

Keywords: Poly(Pentafluorophenyl Acrylate), Post-Polymerization Modification, Antibody-Immobilization, Polymer Brush, Immunoprecipitation, Surface-initiated Reversible Addition-Fragmentation Chain Transfer Polymerization

Student ID: 2014-30262

Contents

List of Figures

List of Tables

Chapter 1. Introduction

1.1. Functional Polymers

Functional polymers are defined as macromolecules that have unique and advanced properties such as optic, electronic, and/or biocompatibility. Since these allow low cost production with facile processing in a wide range of applications such as biotechnology, photonics, and optoelectronics, the studies on functional polymers have been increased. Especially, one of functional polymers, stimuli-responsive polymers have received attention and justified as smart polymers that change their properties or structures in response to external triggers such as temperature,[1,2] pH,[1] light,[3,4] or electric or magnetic field.[5] For example, functional polymeric platforms with desired properties were demonstrated such as thermo-responsive poly (N-isopropylacrylamide) (PNIPAM)[2,6,7] as a nanogel, micelle, and polymer film, or weak polyelectrolyte-based platforms[8-10] like poly(acrylic acid) (PAA),[8] and poly(methacrylic acid),[9] for biosensor or drug delivery. Thermo-responsive polymers have lower critical solution temperature (LCST) or upper critical solution temperature (UCST) which are critical temperature point where polymer and solvent are completely miscible below or above, respectively. Polymer with spiropyran, a photochromic dye, changes its color and wettability on light irradiation.[4] Since functional polymers can convert properties including conformation,[7] adhesiveness,[11]

or water retention,[12] functional platforms comprised of functional polymers are of importance in a wide range of bioapplication,[10, 13] and smart optical system.[14]

As more specific design of polymers for complicated application is required, various synthetic techniques and processing methods have been developed to satisfy demands. The methods of preparing functional polymers can be done by polymerization of functional monomers[15-17] or post-polymerization modification like thiol-ene reaction and click chemistry.[18] In case of polymerization technique, it has been developed to control the chain growth and functionalities delicately using anionic polymerization, controlled radical polymerization such as atom transfer radical polymerization (ATRP), reversible addition-fragmentation chain-transfer (RAFT), and nitroxide mediated polymerization (NMP)), ring-opening metathesis polymerization (ROMP) and Suzuki coupling reaction[19] under palladium catalyst. The technique of post-polymerization modification, especially using activated ester monomers will be introduced in section 1.3.

The functional polymers were tailored to fit particular applications as a structure of aggregates, nanoparticles, films and brushes. The functional polymer films including thin films, membrane, and inorganic hybrid films are enabled to be prepared by spin-casting, drop-casting, dip-coating, layer-by-layer (LbL) method,[20] or block copolymer assembly[21] in the range from nanometer to micrometer scale. Highly fine structures such as polymer brushes can be realized by attachment of polymer chains to the surface or polymerization of monomer from the surface.[22-23] The synthesis and processing methods of functional polymers should be chosen

carefully to materialize the functional platforms.

1.2. Biomolecule Immobilization in Bio-applications

Biomolecule activated organic and inorganic materials have become a new platform of advanced materials with applications in areas such as drug delivery,[24-27] detection of biomolecules,[28-36] and bio-separation.[24, 37-39] While the detailed methods used for the preparation of different bio-materials may differ, they all require the immobilization or attachment of a biomolecule of interest to a material surface.[40-42] The immobilization of biomolecule can occur through physical adsorption [43] via van der Waals forces and/or hydrogen bond formation. Immobilization via covalent bond formation has also been explored.[33, 43-48] In this case, immobilization is achieved by reaction between checmical functional groups expressed on material surface and complementary functionality (typically amine or thiol) present in biomolecules. Lastly, bioaffinity based immobilization[49-51] schemes have also been reported. For example, Protein A/G contains binding domains that can selectively bind to the heavy chain within the Fc region of most immunoglobulins. This antibody-binding property makes Protein A/G an excellent linker material for immobilizing antibody onto material surfaces.[49, 52-54] Regardless of the mechanism of biomolecule immobilization, several common features[55] are considered to be desirable for most applications; 1) high density of biomolecule on material surface; 2) full retention of biomolecule activity after immobilization; and 3) minimized non-specific interaction between biomolecule-activated surface and non-target molecules.

For biomaterial or bio-sensing applications[28-36], the way for immobilization of biomolecules such as antibodies, RNA, DNA, and other proteins to a substrate or other materials have been considered to satisfy some conditions such as high density of immobilized proteins, less nonspecific protein adsorption and full retention of protein conformation and activity.by using diverse functional polymeric materials. Polymers with diverse functional groups were applied to achieve covalent immobilization or crosslinking of biomolecules. Since the attachment of biomolecules to a surface has been regarded as the first step in many bioapplications, the determination of optimal surfaces for each bioapplication is critical.

1.3. Active Ester Monomers and Their Polymers as Precursors for Functional Polymeric Platforms

As already discussed in previous section, the process of difficult design and synthesis of monomer structure, and polymerization is required for giving functionalities on polymer platforms. However, direct polymerization of certain functional monomer is generally limited depending on the tolerance of functional groups under reaction or polymerization condition such as contamination of the initiator or monomer as well as self-polymerization of functional group. To solve the problems and increase the efficiency of polymerization, post-polymerization modification has been suggested and studied due to its convenience of using the prepared polymer for post-modification. Researchers have tried to use hydrogenation,[56] thiol-ene addition,[57] halogenation[58] for post-polymerization modification though low quantitative conversion is achieved even under harsh reaction condition. In order to enhance the efficiency of chemical reactions and reduce the ratio of side product, chemoselective-coupling reaction such as Michael addition,[59] nucleophilic activated cycloaddition,[60] Diels-Alder cycloaddition[61] and activated ester containing monomers was developed.

Activated esters are functional groups with amine-reactivity, which makes the process of functional polymer easier. The concept of activated ester chemistry was first introduced by Ringsdorf[62] and Ferruti[63]. In few decades, diverse monomers containing activated ester moieties were reported such as N-hydroxysuccinimide

(NHS) ester (i.e. N-hydroxysuccinimide acrylate (NHSA) or methacrylate (NHSMA)) or aryl ester with electron withdrawing group (i.e. pentafluorophenyl a acrylate (PFPA) or methacrylate (PFPMA)) (Figure 1). While NHS ester containing monomers have been studied for a long time by plenty of researchers, the major drawback is poor solubility of their polymers in most organic solvent and hydrolytic properties in aqueous solution. In order to find the alternative, various aryl ester with electron withdrawing groups have been intensively studied, especially pentafluorophenyl (PFP) ester-related monomers, which have less toxicity and steric hindrance compared to thrichlorophenyl and pentachlorophenyl ester-based monomer.[64] One of the pentafluorophenyl ester monomers, pentafluoropehnyl acrylate (PFPA) was first reported by Blazejewski and coworkers,[65] but the resulting polymer from polymerization of the monomers was hardly characterized its properties due to insolubility of the polymeric materials.

Patrick and his co-worker have reported the synthesis method of PFPA, and the polymerization using AIBN. Then poly(PFPA) has begun to use in various applications due to its solublity[64] in wide range of organic solvent unlike poly(NHSA) or poly(NHSMA). Based on the characterization of resulting polymers and comparison with many different amine groups and alcohols, PFP ester-based polymers show remarkably high reactivity with primary or secondary amines than the NHS ester-based polymers. Furthermore, acrylate backbones such as PFPA were found to be more reactive than methacrylate counterparts like PFPMA in case of PFP ester based polymers. To fabricate the desired structures and platforms, PFP ester

monomers were polymerized under various living/controlled radical polymerizations such as ring-opening metathesis polymerization (ROMP),[66] reversible addition-fragmentation chain-transfer (RAFT) polymerization,[67] and nitroxide mediated radical polymerization (NMP).[68]

In this thesis, preparation of various functional polymer films and polymer brushes will be introduced by post polymerization modification of PFPA polymerized by RAFT. In chapter 2, post-polymerization modification of simple poly(PFPA)-amine system will be discussed to optimized polymerization condition, which has a potential as a versatile scaffold for realizing various structures. Demonstration of functional polymer brush-grafted particles was studied in chapter 3 and 4, by synthesizing reactive polymer brush platforms and modifying it with various functional molecules and antibodies for specific application. In chapter 5, reactive polymer-coated film was realized as loop or train-shaped brush by silanization with 3-aminopropyl triethoxysilane (APTES), which make amine groups on the surface of substrates. The modified surfaces were applied to the microfluidic channels for biosensing applications.

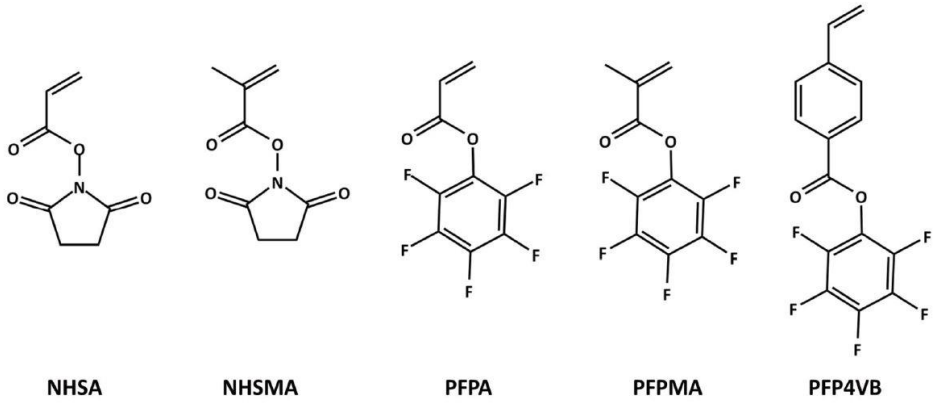

Figure 1 Chemical structures of active ester monomers.

Chapter 2. Reactive Polymeric Platforms Based on Poly(Pentafluorophenyl Acrylate) Polymers

2.1. Introduction

Reactive polymer thin films have recently received substantial attention for many potential applications such as bio-functional membranes[1,2] and stimuli-responsive coatings with controlled wettability.[3,4] Polymers carrying activated ester groups are known to be good candidates due to their high reactivity with primary or secondary amines. One active ester polymer, poly(pentafluorophenyl acrylate) (poly(PFPA)), has been highlighted as a reactive polymer that facilitates the post-polymerization modification. Facile post-modification of pentafluorophenyl esters via amine-containing functional groups allows for convenient and versatile functionalization of diverse polymer platforms including polymer brushes[5,6] and thin films.[7-10]

In particular, the functionalized thin films based on this active ester-amine chemistry have offered an easy approach to realizing diverse functions by simple reactions with quantitative conversion. For example, the post-polymerization modification of poly(PFPA) films with amines has been utilized to obtain free-standing robust fluorescent films by layer-by-layer (lbl) assembly based on covalent bonds between active ester polymers and poly(allyl amine)[10] as well as

functionalized thin films composed of photocleavable block copolymers with a vertically-oriented nanoporous structure.[9] Complete conversion through the entire film thickness was initially inferred by analyzing the components of the films with photoluminescence, NMR or FT-IR spectra. However, very little has been investigated thus far about the exchange mechanism and kinetics of primary alkyl amines applied to poly(PFPA) thin films. To obtain more insights on the post-modification of thin films, an in-depth understanding of the internal structural changes of polymer films triggered by active ester-amine chemistry was required for practical applications.

Herein, we report the detailed internal structural changes in the amine-treated poly(PFPA) thin films as a function of the aliphatic chain length of the primary amines as well as the molecular weight of the poly(PFPA).[11] The poly(PFPA) thin films investigated in this study were prepared in the form of spin-cast thin films. Because the spin coating method has the ability to quickly and easily produce well-defined films,[12,13] the spin-cast thin films of poly(PFPA) could be used as model systems. In addition, the interactions between solvent and polymer films have primarily been studied to gain insights regarding polymer film systems in the case of solution processes, such as the penetration of solvent molecules and the dissolution behavior of polymer thin films.[14-16] Similarly, it is important to monitor the status of functionalized poly(PFPA) films because post-polymerization modification should be performed in an amine-containing solution.

Thin films of high and low molecular weight poly(PFPA) synthesized by

reversible addition-fragmentation chain transfer (RAFT) polymerization were treated post-polymerization with simple primary alkyl amines of different alkyl chain lengths. We conducted quartz crystal microbalance with dissipation (QCM-D) monitoring to determine the amine-exchange kinetics *in situ* and in real time, combined with atomic force microscopy (AFM) and optical microscopy (OM) to observe the changes in the surface morphology. Furthermore, the changes in the film thickness and internal structure of poly(PFPA) films after amine-treatment were observed with neutron reflectivity (NR) measurements, which are regarded as a powerful tool to study the material interfaces in nanometer-scale thin films.[13]

2.2. Experimental Section

Materials. All chemicals and solvents were purchased from Sigma-Aldrich and used as received, except for acryloyl chloride, which was purchased from the Tokyo Chemical Industry Co., Ltd. Benzyl dithiobenzoate (BDB), used as the RAFT chain transfer agent, was synthesized according to a previously published method.[17] Silica gel for column chromatography was purchased from Merck Chemical Company. Silicon wafers (100) and Au sensor crystals (QSX 301, Q-Sense) were used as substrates to prepare the polymer thin films.

Synthesis of Pentafluorophenyl Acrylate (PFPA). Pentafluorophenol (15.3 g, 83.1 mmol) and 10.0 g (98.8 mmol) of triethylamine (TEA) were dissolved in 150 ml of diethyl ether, and 8.95 g (98.9 mmol) of acryloyl chloride was added dropwise through a funnel under cooling with an ice bath. The solution was stirred for 1 h in an ice bath and then stirred overnight at room temperature. After the precipitated salt was separated by filtration, the solvent was evaporated, and the crude product was purified by column chromatography (column material: silica gel; solvent: petroleum ether). A colorless liquid (15.8 g, 66.4 mmol, 80 %) was obtained. 1H NMR (CDCl3): δ/ppm: 6.74 (d, 1H), 6.39 (dd, 1H), 6.19 (d, 1H). 19F NMR (CDCl3): -161 (d, 2F), -156.70 (t, 1F), -151.40 (d, 2F). FT-IR: 1772 cm-1 (C=O ester band), 1516 cm-1 (C=C aromatic band). The detailed procedure has been well-documented in previous studies.[18,19]

Synthesis of Poly(PFPA) via RAFT Polymerization. A 1.13 g (4.72 mmol) aliquot of PFPA, 5.0 mg (0.0205 mmol) of BDB, 0.4 mg (0.00244 mmol) of 2,2'-azobis(2-methylpropionitrile) (AIBN) and 3.0 ml of anisole were placed into a Schlenk flask. After three freeze-pump-thaw cycles, the flask filled with nitrogen gas was stirred in an oil bath at 70 ℃ for 4 h and then cooled down to room temperature. The polymer was precipitated into methanol twice and dried in a vacuum oven. 1H NMR (CDCl3): δ/ppm: 3.10 (br, s), 2.5 (br, s), 2.13 (br, s). 19F NMR (CDCl3): -164 (br, s), -158.6 (br, s), -155 (br, s).

Poly(PFPA) Thin Film Preparation and Post-Treatment with Primary Alkyl Amines. Silicon wafers (100) were cleaned using piranha solution (70 % H2SO4 and 30 % H2O2) for 20 min, rinsed with deionized water, and dried with a nitrogen stream. Poly(PFPA) thin films were deposited by the spin-coating method using 3 wt% of poly(PFPA) solution in tetrahydrofuran (THF) with a spin-rate of 3000 rpm for 30 s. High (Mw = 170 kg/mol) and low molecular weight (Mw = 37 kg/mol) poly(PFPA) thin films were prepared, and post-polymerization modification was performed by dipping the films in a 1 wt% solution of primary alkyl amine. Each alkyl amine with a different alkyl chain length (amylamine and dodecylamine) was dissolved in ethanol. The post-polymerization treated films were washed thoroughly with ethanol, and all films were dried under a stream of nitrogen.

Characterization. ^{1}H NMR spectra and ^{19}F NMR spectra were recorded on a Bruker Avance 500 MHz FT-NMR spectrometer. Chemical shifts were given in ppm relative to trimethylsilane (TMS). Gel permeation chromatography (GPC) was used to determine the molecular weight and the corresponding polydispersity index (PDI = M_w/M_n) of the polymer samples. GPC (YL9100, Young Lin Instrument Co. Ltd.) measurements were performed under poly(styrene) standards in THF with a 5 mg/ml polymer sample concentration.

The film thickness was obtained by a variable-angle multiwavelength ellipsometer (Gaertner L2W15S830, Gaertner Scientific Corp.). The film surface morphology was monitored by tapping-mode atomic force microscopy (AFM, Veeco, Innova) combined with an optical microscope. Every film treated with amines for a specific reaction time (0, 20, 40, and 60 min) was characterized under air after thorough washing with ethanol followed by gentle drying with a nitrogen stream.

The QCM-D measurements (Q-Sense D300, Q-Sense) were performed to monitor the changes in frequency (Δf_n) and dissipation energy (ΔD_n) of an Au sensor crystal (QSX301) coated with poly(PFPA) during the chemical reaction. The changes in frequency (Δf_n) are proportional to the changes in mass, according to the Sauerbrey equation.[20] The dissipation energy shift (ΔD_n) indicates the loss of energy stored in the vibration cycle, which yields useful information on the changes in the viscoelastic properties as well as the structural transformation.[12,13] As-prepared poly(PFPA) films were immersed in a poor solvent, ethanol, for 1 hr in order to set

the baseline to monitor the amine-treated changes in the QCM frequency and dissipation energy in the solvent setting. After the stabilization, 0.5 ml of amine solution was injected into the sample chamber. The applied voltage was sequentially pulsed across the Au sensor crystal, allowing the shear wave to dissipate as well as the simultaneous measurement of the absolute dissipation and absolute resonant frequency of the crystal for all four overtones (n = 1, 3, 5 and 7, i.e., 5, 15, 25, and 35 MHz). All of the measurements were taken at 25 °C. Because Δf_1 and ΔD_1 were typically noisy due to insufficient energy trapping, the frequency changes in the third overtone ($\Delta f_3/3$) were compared between the samples.

The internal structures of post-treated poly(PFPA) films were characterized by NR. Samples for NR experiments were prepared on 3 in. diameter and 5 mm thick silicon wafers. All measurements were performed at room temperature. NR measurements were conducted with a vertical reflectometer at the High-flux Advanced Neutron Application Reactor (HANARO) of the Korea Atomic Energy Research Institute in Daejeon, Korea. The neutron wavelength (λ) was 4.75 Å, with $\Delta\lambda/\lambda$ equal to approximately 0.02. Scattering from samples was corrected for background, and the reflectivity curves were fitted to obtain the depth profile by using Parratt 32 and Motofit reflectivity analysis packages. The resulting scattering length density (SLD) profiles defined the zero of film thickness as the interface between a polymer and a native oxide layer. The film thickness was calculated based on the model layers of polymer films.

2.3. Results and Discussion

2.3.1. Post-Modification of Poly(PFPA) Thin Films with Primary Alkyl Amines

Poly(PFPA) was synthesized by RAFT polymerization with a desired molecular weight (M_W = 37 kg/mol) and a relatively narrow polydispersity index (PDI = 1.3). Additional functionalization process of the poly(PFPA) thin films is triggered by aminolysis reaction with primary alkyl amines dissolved in ethanol, which is classified as a poor solvent for poly(PFPA). The aminolysis reaction of the poly(PFPA) with primary alkyl amines is presented in Figure 2. In order to understand the post-modification process of poly(PFPA)films (M_W = 37 kg/mol) with dodecylamine ($CH_3(CH_2)_{11}NH_2$) solution, we monitored the changes in film thickness as well as in surface morphologies as a function of post-treatment time. Figure 3 shows that the thickness of post-treated films slowly increases at the early stage, followed by a rapid decrease in film thickness. The initial spin-cast poly(PFPA) films have relatively smooth (rms roughness = 0.20 nm) and flat surfaces before the post-treatment. However, the film surfaces gradually develop irregular patterns of droplets as the dipping time of the films in amine solution was increased (Figures 4).

Polymer dissolution in good solvents is composed of the following common stages in sequence: the penetration of solvent molecules into polymer films leading to the relaxation of polymers, the formation of a solvent-swollen gel layer, and the diffusion of polymer chains into solvent.[16] Although ethanol is a poor solvent for

poly(PFPA), the films show the ordinary dissolution behavior in a good solvent during the post-treatment with dodecylamines. This indicates that the amine molecules used as substituents change the solubility of polymer chains during the post-polymerization modification in ethanol solution. We can make a hypothesis that the amine molecules penetrate into the excluded volume of poly(PFPA) films and form a swollen amine-substituted polymer gel layer, which finally leads to the dewetting behavior followed by dissolution in ethanol. Also, the substitution of pentafluorophenyl groups in poly(PFPA) with amine moieties occurs directly after the penetration of amines and solvent molecules due to the high reactivity of poly(PFPA) with primary amines. However, the further studies are needed to clearly elucidate the detailed mechanism on the penetration and substitution of amines in poly(PFPA) films as well as the swelling and dissolution of resulting poly(N-alkyl acrylamide) films in solution state. In this regard, we studied the post-modification kinetics of the poly(PFPA) film as a function of aliphatic chain length of the primary alkyl amines.

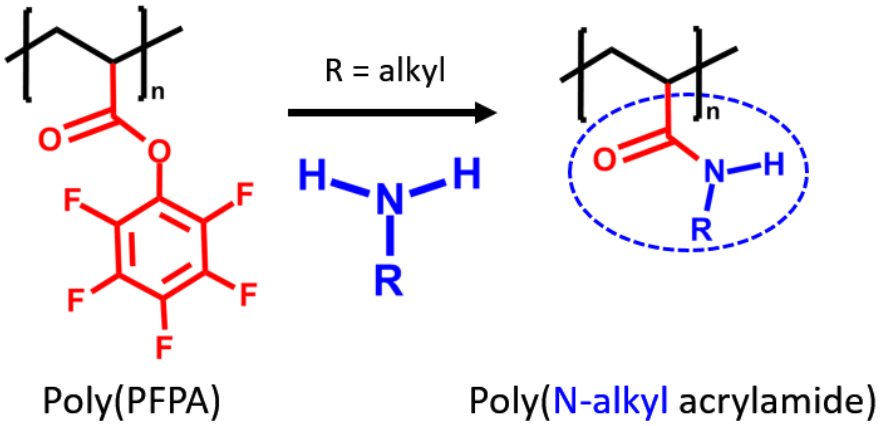

Figure 2 Chemical structures of reactive poly(PFPA) and primary alkyl amine. The amynolysis reaction results in the product (poly(N-).

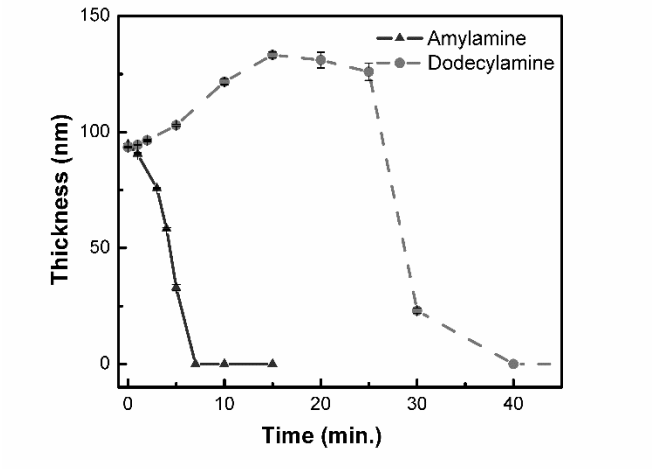

Figure 3 Thickness changes in poly(PFPA) films (MW: 37 kg/mol) post-treated with amylamine (solid) and dodecylamine (dash).

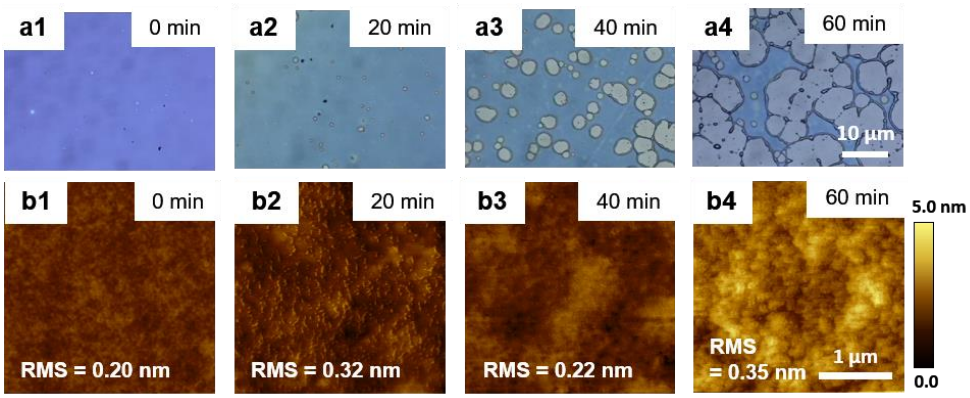

Figure 4 (a) Optical microscope images and (b) tapping mode AFM height images of poly(PFPA) films (M_W = 37 kg/mol) after 0 (a1, b1), 20 (a2, b2), 40 (a3, b3) and 60 min (a4, b4) treatments with dodecylamines. AFM images were obtained from the areas where no dewetting was observed.

2.3.2. Effect of Aliphatic Chain Length of Primary Alkyl Amines on the Exchange Kinetics of Poly(PFPA) Films

We monitored the changes in surface morphology during the post-modification with amylamine containing 5 carbons ($CH_3(CH_2)_4NH_2$) in order to examine the effect of aliphatic chain length on the substitution kinetics to reactive groups in the poly(PFPA) thin films (M_W = 37 kg/mol), as compared to the treatments with dodecylamine.

The poly(PFPA) films treated in amylamine solution for 10 min revealed the bare silicon wafer due to the facile diffusion of the resulting amine-substituted polymers in ethanol. On the other hand, dodecylamine-treated poly(PFPA) films remained on the silicon wafers after the same post-treatment time (10 min) while showing small holes in the swollen state, as confirmed by the increase in film thickness as well as surface morphologies (Figures 5a-b). This indicates that the shorter primary alkyl amines induce much faster exchanges with pentafluorophenyl side groups in the polymers leading to faster dissolution of poly(PFPA) films when compared with longer primary alkyl amines. This result suggests that we can tune the exchange kinetics of poly(PFPA) films by using primary alkyl amines with different aliphatic chain length.

To elucidate the detailed mechanism on the swelling and dissolution kinetics of poly(PFPA) films treated with two different types of amines, we performed quartz crystal microbalance with dissipation (QCM-D) monitoring as

shown in Figure 6a-b. Amylamine quickly reacted with pentafluorophenyl groups of poly(PFPA) films as soon as amylamines dissolved in ethanol was injected into a QCM-D cell containing a poly(PFPA)-coated substrate. Initial negative frequency shift of the amylamine-treated film indicates a small gain in mass, which originates from the binding of amylamines to the polymer in such a short time (Figure 6a). After the quick substitution of the amines into poly(PFPA) films, they rapidly form poly(N-pentyl acrylamide) that is readily soluble in ethanol, resulting in the successive loss in mass, as confirmed by a significant increase in frequency shift after 10 min of treatment.

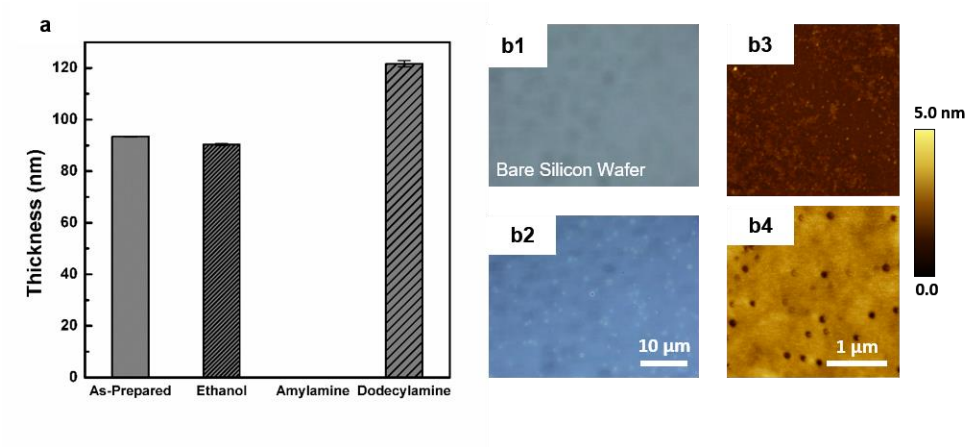

Figure 5 (a) Thickness of poly(PFPA) film (MW: 37kg/mol) as-prepared and films immersed in ethanol, amylamine-ethanol solution, and dodecylamine-ethanol solution in 10 min. (b) Optical microscope and AFM images of poly(PFPA) films after 10 min treatment with amylamine (b1, b3) and dodecylamine (b2, b4).

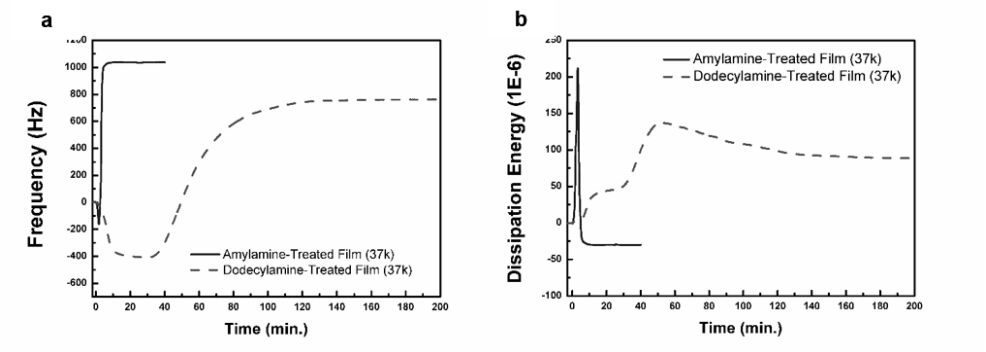

Figure 6 QCM-D monitoring on the changes in (a) frequency and (b) dissipation energy of poly(PFPA) films (37 kg/mol) post-treated with amylamine (line) and dodecylamine (dash).

In addition, the initial rapid increase in the dissipation energy demonstrates the formation of swollen layers on the top film surface (Figure 2d). The amylamine molecules quickly penetrate into the poly(PFPA) films and the interactions between the reacted polymer chains and ethanol become more favorable. We note that the kinetics in QCM-D results correspond to the time-scale of the changes in surface morphologies made by AFM, which supports the rapid penetration and spontaneous substitution of amylamines into the modified film, triggering quick dissolution of the film.

On the other hand, in the case of the post-treatment with dodecylamines with 12 carbons in the alky chain, QCM-D curves demonstrate much slower penetration and dissolution kinetics due to the longer retention time of a swollen polymer gel layer. Dodecylamines slowly penetrated into the films for 20 min due to its bigger size while amylamine soaked into the films quickly. The mass of dodecylamine-treated polymer films gradually increased during the initial 15 min of treatment. We believe that this is because the excluded volume of the polymer layer was gradually increased as dodecylamines and solvent molecules slowly penetrated into the films. Besides, it is observed that the dodecylamine-treated film represents the two-step-increase in dissipation energy. This indicates that dodecylamines could not readily penetrate into the film but are adsorbed on the surface upon reaction at the initial state, developing soft top layers interacting with ethanol solvent. After the slow propagation of the swollen layer into the entire film by the full sorption of dodecylamines for 40 min, the dodecylamine-modified polymer layers start to

dissolve in ethanol. Also, the QCM-D result exactly corresponds to the results of film thickness and surface morphology: the initial increase in film thickness due to the adsorption of dodecylamines at 10 min, the growth of holes on the film surface at 40 min, and the resulting dewetting at 60 min, as shown in Figures 4.

From the observed changes in poly(PFPA) film mass, softness, film thickness and surface morphologies as a function of treatment time with different amines, we have traced the detailed post-modification mechanism of reactive poly(PFPA) films with primary alkyl amines. In addition, we have clearly demonstrated that the kinetics in this sequential reaction can be regulated by the aliphatic chain length of substituting primary amines. The longer primary amines lead to slower penetration and substitution rate in well-defined spin-cast poly(PFPA) films when compared with the shorter amine counterpart. The dewetting and dissolution kinetics can also be delayed as the aliphatic chain length of primary amines is increased. Since ethanol is a poor solvent for poly(PFPA), the spin-cast poly(PFPA) films have very well-defined and tightly collapsed surfaces in contact with pure ethanol. But, once amine molecules reach or contact the film, amines penetrate into the films and undergo the substitution reaction altering the solubility of the film in ethanol. In the penetration and substitution steps, it is noted that the size of primary amines critically determines the formation rate and the solubility of the substituted poly(N-alkyl acrylamide).

Nevertheless, the ultimate dissolution of polymer thin films after the post-treatment makes it hard to utilize and functionalize poly(PFPA) thin films by using the easy substitution with functional primary alkyl amines. Furthermore, more

information on the control of penetration depth of amines and the degree of substitution is required to realize functional surfaces. Hence, in order to identify physical parameters to tune the degree of substitution of amines into poly(PFPA) thin films as well as to prevent the dissolution of amine-modified films, we further investigated the effect of molecular weight of poly(PFPA) on the dissolution.

2.3.3. Effect of Molecular Weight of Poly(PFPA) Chains on the Dissolution of Poly(PFPA) Thin Films Post-Treated with Primary Amines

Molecular weight of polymer films is another important physical parameter to control the degree of functionalization of poly(PFPA) films. Two different poly(PFPA) with low (M_w = 37 kg/mol) and high (M_w = 170 kg/mol) molecular weights were synthesized to investigate the molecular weight effect on the post-modification with simple aliphatic amines. Along with the kinetics obtained from QCM-D measurements, neutron reflectivity (NR) was additionally employed to gain information on the internal structural changes of films after amine-triggered post-treatment. NR is the most advantageous tool to investigate buried structure and interfacial roughness in nanometer-scale within a polymer thin film, which contains strong neutron scattering contrast layers. Since the scattering length density (SLD) of poly(PFPA) is much higher than that of amine-modified poly(N-alkyl acrylamide) due to neutron-rich pentafluorophenyl side groups ($SLD_{poly(PFPA)}$ = 3.5~3.8×10^{-4} nm^{-2}, $SLD_{poly(N\text{-}alkyl\ acrylaminde)}$ = 0.3~0.6×10^{-4} nm^{-2}), we can obtain enough information on the penetration depth of amines into the film as well as the resulting swollen polymer gel layer thickness of poly(N-alkyl acrylamide) without additional deuteration of polymers for NR measurements.

We demonstrated that poly(PFPA) films of lower molecular weight (M_w = 37 kg/mol) show distinctly different kinetics in post-modification reaction according to

the aliphatic chain length of primary amines. NR measurements have been conducted to analyze the component changes in the polymer films before and after the post-treatment as a function of molecular weight of poly(PFPA) and aliphatic chain length of primary amines. In order to prove the detailed post-modification mechanism suggested by QCM-D, microscopy and thickness monitoring, the internal structures of the films were systematically investigated by NR at specific post-treatment time (0, 3, 5, and 10 min), which were selected from the swelling time region identified in the QCM-D experiments (Figure 7).

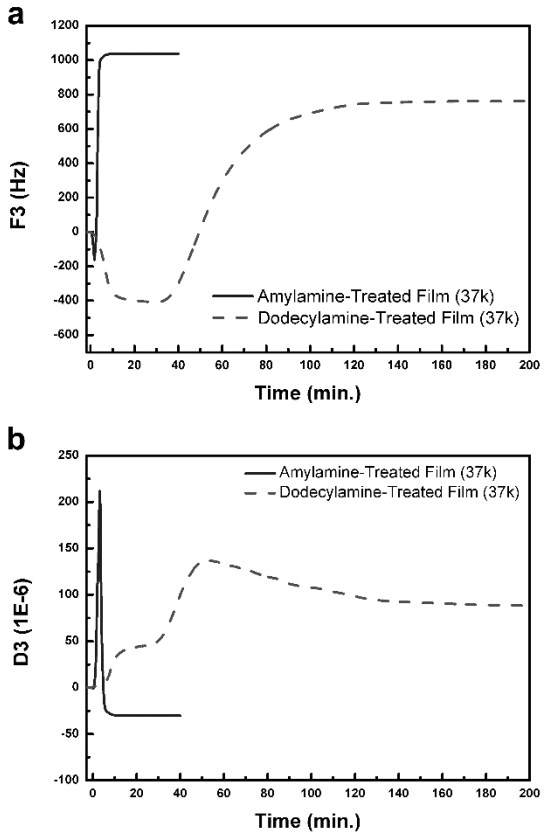

Figure 7 QCM-D monitoring on the changes in (a) frequency and (b) dissipation energy of poly(PFPA) films (37 kg/mol) post-treated with amylamine (line) and dodecylamine (dash).

As shown in Figure 8a, the SLD values of amylamine-treated films significantly decrease as the treatment time is increased, demonstrating that amylamine molecules vigorously penetrate into the low molecular weight films (M_w = 37 kg/mol). After 5 min treatment with amylamines, total thickness of the post-treated film reduced to 24.7 % (73.3 nm) of original film thickness (97.5 nm). The amylamine molecules penetrated into 40.8 % of initial film thickness after 5 min of treatment, which was estimated from the ratio of thickness of remained poly(PFPA) layer (57.7 nm) with respect to the original film thickness. Since the penetration of amine molecules triggers the decrease in SLD value from the polymer-air interface, the layer of unreacted poly(PFPA) was defined as the layer which has the SLD value of poly(PFPA) ($3.5\sim3.8\times10^{-4}$ nm^{-2}), calculated from the fitted model layers. The approximate degree of functionalization of poly(PFPA) films is estimated from the SLD reduction (%), the percentage ratio of the area under the SLD curves of as-prepared and post-treated polymer films. The SLD reduction originates from the substitution of pentafluorophenyl groups to N-pentyl groups that has much lower SLD value. From this point of view, 25.4 % of SLD reduction of 5-min treated film implies quantitative changes in the internal components. In addition, the low molecular weight polymers with reactive side groups that were exchanged with amylamines were rapidly dissolved into ethanol from the top film surface within approximately 10 min. After 10 min, only 5.3 nm thickness of polymer films is left with the 0.3 nm thickness of unreacted poly(PFPA), resulting in SLD reduction up to 93.4 %. The changes in film structure and internal components of the amylamine-

treated low molecular weight film occur so rapidly due to the fast penetration and exchange kinetics of short amylamines as well as the rapid dissolution of the resulting low molecular weight poly(N-pentyl acrylamide).

The results with higher molecular weight (M_w = 170 kg/mol) poly(PFPA) films are reasonable to investigate the interpenetration depth profile of amylamines into the poly(PFPA) films with NR, which allow us to understand exactly what happens inside the film (Figure 8b). The amylamine-treated high molecular weight polymer films maintain the total film thickness while demonstrating the amine penetration depth and the interlayer roughness as a function of post-treatment time in the fitted SLD profiles. Poly(PFPA) chains of high molecular weight were almost intact at the top film surface even after the exchange with alkyl amines, which was confirmed by the fact that there was virtually no significant change in the film thickness of the poly(PFPA) film in the SLD curve after the post-treatment for 10 min. However, amylamine molecules gradually penetrate into the film. As a result, the exchanged product poly(N-pentyl acrylamide) is formed as a swollen gel layer, but this dissolves much more slowly into ethanol due to the increased entanglements between longer polymer chains. In the same vein, 5 min-treated poly(PFPA) films have 45.8 nm of amine-functionalized layer, which means that 36.5 % of the initial film thickness was penetrated by amylamine, accompanied with 25.4 % of SLD reduction. For the additional 5 min of treatment, the SLD reduction increases up to 42.3 %, accompanied by 50.8 % of the amine penetration depth into the film, while the dry film thickness of poly(PFPA) films slightly changes from 134.8 nm (5 min)

to 120.5 nm after 10 min of treatment (i.e., 3.7 % and 13.9 % decrease with respect to the original film thickness (140.0 nm)).

When we compare the data of 5 min treatment with amylamine between two different molecular weight polymer films, 40.8 % of amylamine penetration depth in the low molecular weight polymer film is similar to 36.5 % of that in the high molecular weight film. However, the film thickness of the low molecular weight film is significantly decreased (24.7 %) when compared with a slight drop (3.7 %) in the film thickness in the case of high molecular weight film. That is because that the dissolution behavior of the low molecular weight polymer film is accelerated by the instant swelling of the exchanged layer. On the other hand, the high molecular weight polymer films could maintain the whole thin film structure even after post-treatment with amylamines. These results indicate that short primary amines can readily penetrate into polymer films regardless of the molecular weight of polymers, whereas the dissolution of amine-modified polymer films is wholly dependent on the polymer molecular weight.

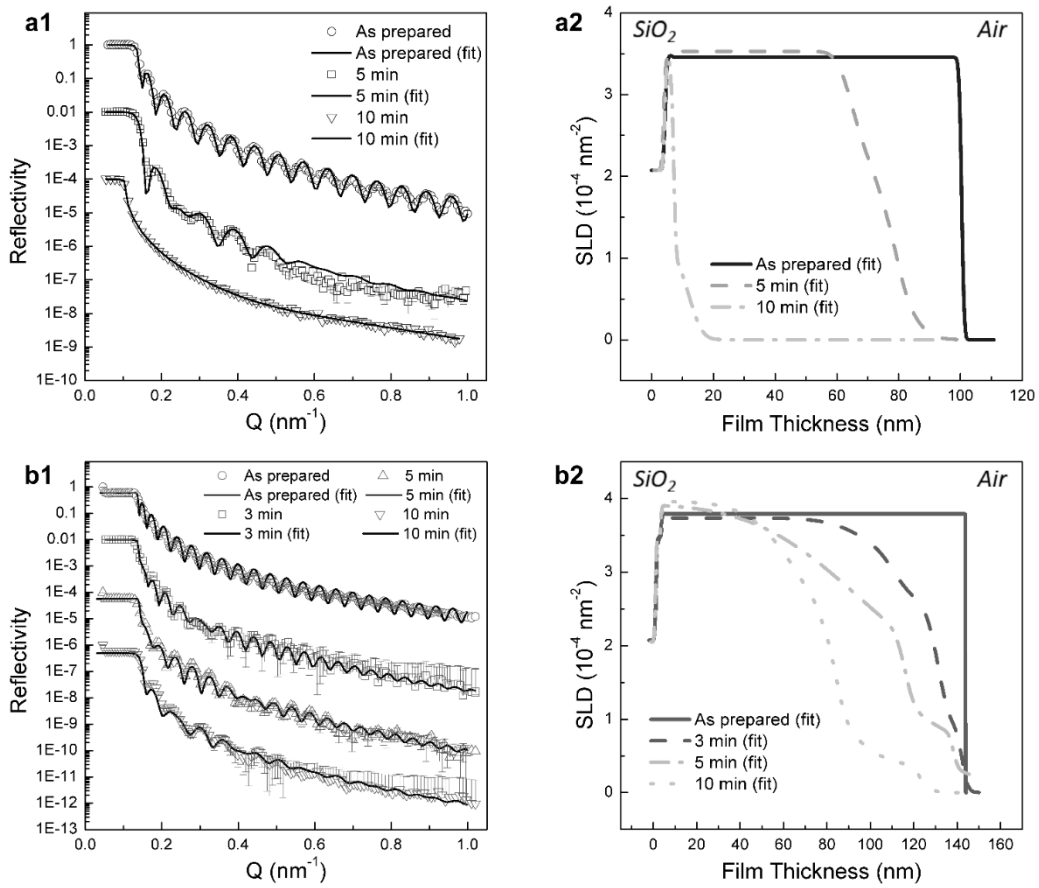

Figure 8 Neutron reflectivity curves and SLD profiles of as-prepared and post-treated poly(PFPA) films of (a) low molecular weight (37 kg/mol) (b) high molecular weight (170 kg/mol) after amylamine-treatment with different times.

Contrary to the amylamine modification, the post-treatment with dodecylamines shows the different behavior in penetration and exchange in poly(PFPA) films as well as the different dependency on polymer molecular weight. As shown in Figure 9a-b, QCM-D data demonstrate that the high molecular weight polymer film shows the increase in mass and the development of a soft layer at the top surface due to amine binding and the formation of swelling layer, while the low molecular weight film is finally dissolved into ethanol after amine penetration. It is also noted that the dodecylamine treated low molecular weight film has an equilibrium in the swelling region from 20 to 40 min before disintegration while the high molecular weight film does not dissolve even after swelling with amine exchange.

The fact that dodecylamine has the lower diffusion rate than amylamine makes the noteworthy difference in the SLD profiles as a function of post-treatment time. Compared with the penetration profiles of amylamine, dodecylamine molecules are soaked into the poly(PFPA) film in much slower rate and dodecylamines that could not rapidly penetrate in a short time are simply bound to the surface regardless of polymer molecular weight. The swollen layer of dodecylamine-treated polymers yielded the increased film thickness in both molecular weight cases because of its longer alkyl chain moieties. Nonetheless, the final dissolution behavior of the product in ethanol is determined by the molecular weight.

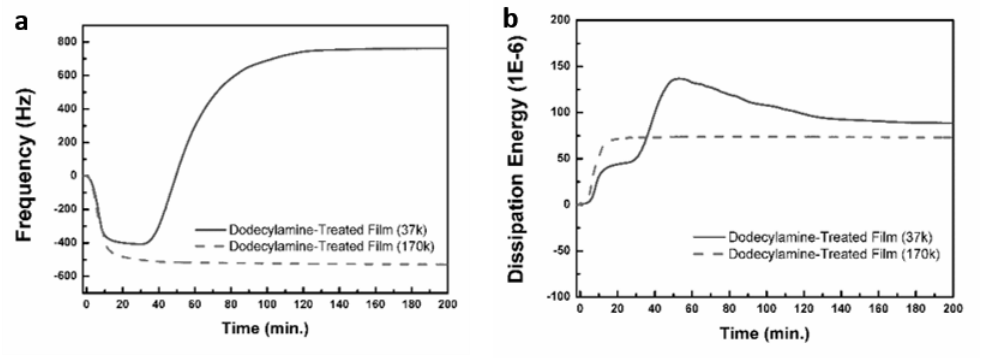

Figure 9 QCM-D data showing the changes in (a) frequency and (b) dissipation energy of poly(PFPA) films with low (37 kg/mol; solid line) and high (170 kg/mol; dashed line) molecular weight post-treated with dodecylamines.

In more detail, poly(PFPA) thin films of low molecular weight (M_w = 37 kg/mol) had a retardation in the penetration rate of dodecylamines, but the exchange process finally led to the complete dewetting of the films. Figure 10 indicates the formation of a swollen layer after 10 min of treatment with an increased film thickness, 29.4 % increase with respect to the original film thickness (97.5 nm). Fitted model layers of the NR curves show that dodecylamine penetrated 19.2 % of the initial film thickness, estimated from the thickness of unreacted poly(PFPA) (78.8 nm) and 5.4 % reduction of SLD value. However, the dewetting eventually occurred after the films were fully exchanged with amines and swollen, as noticed from the QCM-D data. Poly(PFPA) films of low molecular weight after longer treatment time with dodecylamine cannot be measured with NR due to severe roughening of the surfaces of polymer films.

On the other hand, the dissolution process is apparently limited in the high molecular weight polymer film even after forming the top swollen layer consisting of poly(N-alkyl acrylamide). As shown in Figure 11, the thickness of post-treated films slightly increased 11.9 % (156.2 nm) of the original thickness (140.0 nm). Despite the increase of the total film thickness, SLD value reduced up to 21.3% in the whole film, demonstrating dodecylamine penetrated 37.1 % of the initial film thickness. Even after the first 10 min of treatment, most of amine-functionalized polymer chains remained in the polymer matrix with the continuous increase in the thickness of the swollen layer at the surface. At the same reaction time, dodecylamine molecules can penetrate more deeply into the polymer film when the

film is composed of higher molecular weight poly(PFPA). The increase in the film thickness is induced by the reaction of dodecylamines with poly(PFPA) chains and the corresponding formation of longer alkyl side chains. The entanglements of high molecular weight polymer chains within the thin film also prevent the dissolution of the polymers after the aminolysis reaction.[21] Also, it has been well documented that the tightly packed surfaces of spin-cast films have also an important role to control the degree and rate of penetration and dissolution of solvent as a function of molecular weight.[13] This indicates that amine-modified functional polymer thin films can be simply realized by the aminolysis reaction of high molecular weight poly(PFPA) films by soaking functional amines dissolved in solvent. Moreover, it is concluded that the penetration depth of amines and the corresponding degree of functionalization in high molecular weight reactive thin films can be controlled by the aliphatic chain length of primary amines.

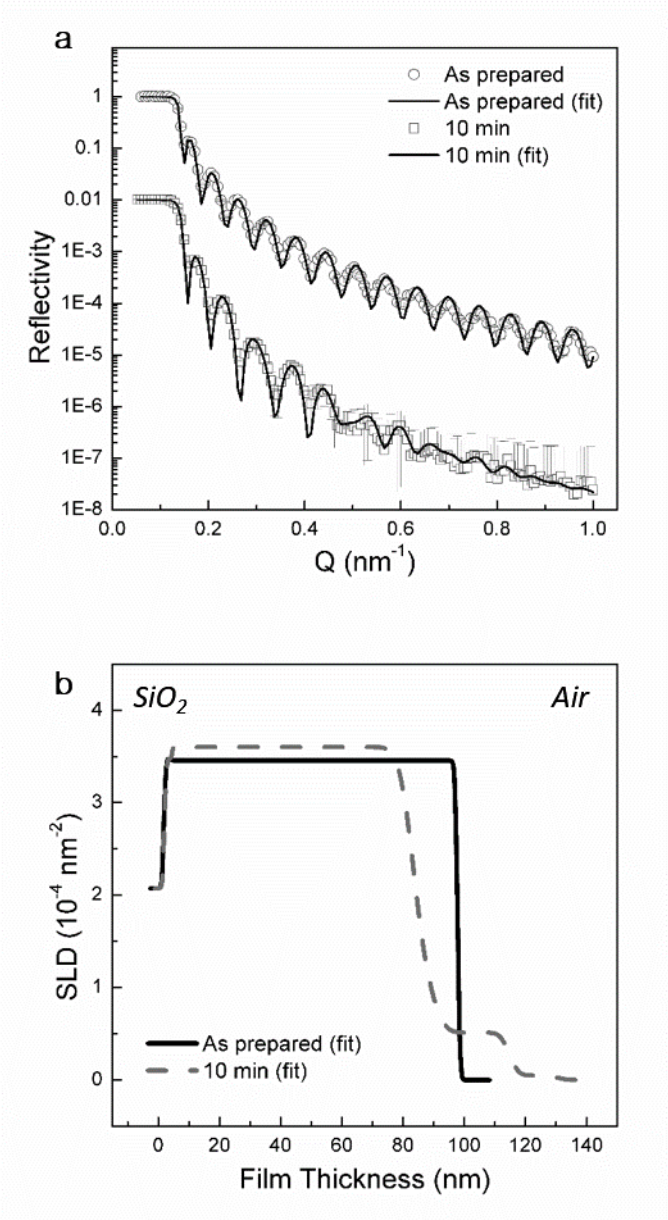

Figure 10 Neutron reflectivity curves (a) and SLD profiles (b) of as-prepared and post-treated poly(PFPA) films of low molecular weight (37 kg/mol) after treatment with dodecylamines.

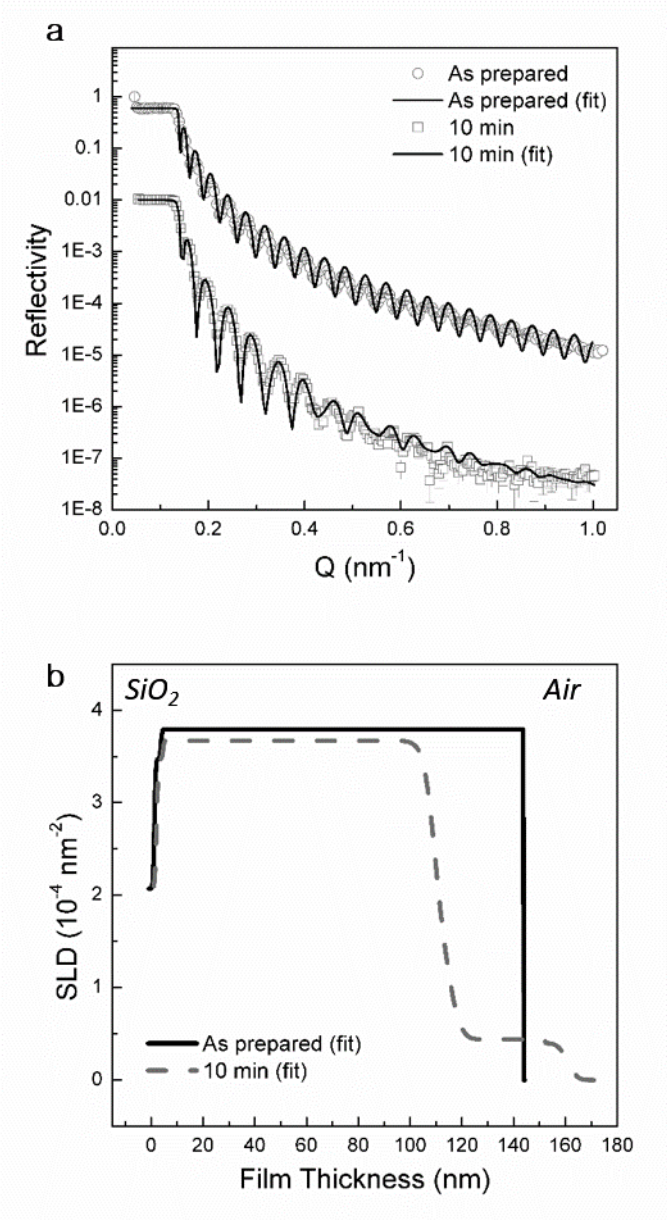

Figure 11 Neutron reflectivity curves (a) and SLD profiles (b) of as-prepared and post-treated poly(PFPA) films of high molecular weight (170 kg/mol) after treatment with dodecylamines.

2.3.4. NR Studies on the Amine-Exchange Kinetics of Poly(PFPA) Films

Based on the observation of surface morphologies in nanometer- and micrometer-scale, film mass and softness, and internal layered structures, we identify the size of primary alkyl amine as a new factor between the disentanglement of initial polymer thin film and the solvent diffusion, which are important parts of the dissolution of polymer.[16] The post-modification process in the poly(PFPA) films with primary alkyl amines is conducted through three main steps: adsorption and penetration of amine and solvent molecules, aminolysis reaction, and the diffusion or dissolution of resulting poly(N-alkyl acrylamide) chains into solution(Figure 12). The degree of amine penetration as well as the modification rate can be tuned by the size of alkyl length in amine molecules, while the dissolution kinetics is mainly controlled by the molecular weight of reactive polymers leading to backbone structure in thin films. Consequently, high molecular weight of reactive poly(PFPA) films has a great potential for controlled post-modification via functional amines without loss of films in a treatment solution.

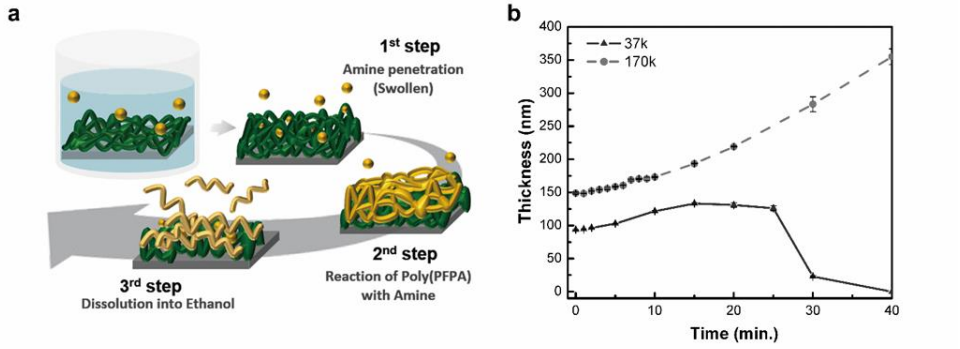

Figure 12 (a) A schematic description on the process of post-modification of poly(PFPA) films with amine. (b)Thickness changes in poly(PFPA) films of low molecular weight (37 kg/mol; solid) and high molecular weight (170 kg/mol; dash) post-treated with dodecylamine. In this case, the dissolution behavior of the high MW films did not occur.

2.4. Conclusion

The spin-cast poly(PFPA) films were subject to post-polymerization modification based on the fast reactivity with primary amines. Either amylamines or dodecylamines, with different alkyl chain length, were used for the post-modification of the poly(PFPA) thin films. The results demonstrated that amine molecules penetrate into the films from the top surface making the films swollen due to high affinity between amine-modified polymers and solvent (ethanol). The rate of amine penetration and exchange in poly(PFPA) films was mostly determined by the aliphatic chain length of primary amines employed for the post-treatment. Longer alkyl length of primary amines led to the slower penetration and exchange process in the poly(PFPA) films. It was also observed the short amylamine-modified polymer films with low molecular weight were rapidly dissolved into solvent. However, the dissolution behavior of amine-treated polymer films could be reduced with the increase in the molecular weight of poly(PFPA) in thin films. As a consequence, we could easily realize the amine-functionalized thin films through spin-casting of high molecular weight poly(PFPA) films and immersing it in amine-containing ethanol solution for 10 min without the dissolution of the polymer films. This fundamental study that demonstrates the effects of aliphatic chain length in primary amines as well as the molecular weight of reactive polymers would provide important physical parameters for the functionalization of polymer thin films based on the chemical substitution of side groups performed in a solvent. Furthermore,

based on the fundamental information provided in this study, the reactive poly(PFPA) thin films would be further extended into diverse functional platforms through versatile post-modifications with a number of amines that have different functionalities.

Chapter 3. Preparation of Poly(Pentafluorophenyl Acrylate) Brush-Grafted on Silica Particles

3.1. Introduction

Polymer brushes are functional polymer chains tethered, at one end, to an interface or a solid surface.[1] Polymer brushes can be prepared by physiosorption or chemisorption of polymer chain by a grafting to method or polymer grows from surface by a grafting from method. When the polymer chains are grown from initiator on the surface, polymer brushes with high density can be obtained which lead to extreme chain stretching due to steric repulsion.[2-3] Polymer brush has been used extensively in areas such as antibacterial surface,[4] cell adhesion,[5] protein immobilization,[6] biosensor[7-8], responsive polymer,[9-10] and charge transfer layer[11-12] depending on functionality.

The structure of a surface-immobilized polymer can be evaluated by the inverse value of the distance between grafting points (D) and film thickness (h) (Figure 4.1).[13] The point where the size of grafted polymer chains approaches the distance between grafting points is called as a transition point between a single grafted chain (mushroom) regime and brush regime. A commonly used literature parameter for quantitative characterization of this transition is the reduced tethered density (Σ) or more simply grafting density (σ), defined as equation (3.1and 3.2).[2]

$$\Sigma = \sigma\pi R_g^2 \quad \text{Equation 3.1}$$

$$\sigma = h\rho NA/M_n \quad \text{Equation 3.2}$$

R_g is radius of gyration of a tethered chain at specific experimental conditions of solvent and temperature. h is film thickness, ρ is bulk density of the brush composition, and Na is Avogadro`s number. Literature grafting density of high-density brushed is around 0.7, it of semi-dilutes brush is 0.05, and it of mushroom is less than 0.01.[2]

Surface initiated polymerization of brushes were demonstrated by various controlled radical polymerization techniques such as ATRP,[14] RAFT,[15] ROMP,[16] NMP[17] to maximize the control over grafting density, polydispersity, and composition. Polymer brushes with desire functions can be realized by surface initiated polymerization of functional monomers or post polymerization of pre-polymerized polymer brushes. The former required difficult synthesis of monomers and is often tedious for optimizing polymerization conditions for each monomer. Furthermore, due to tolerance, some functional monomers have limitation on polymerization. The latter is of special interest as platforms for various functional brushes with hydroxyl-, carboxylic acid-, and carboxylic ester-groups. Those functional groups, however, can be only modified with limited chemicals under harsh or toxic environment and have limitation on conversion and control.

Recently, a new type of activated ester, the pentafluorophenyl, or PFP ester, is receiving attention due to its high reactivity with amines along with their enhanced

resistance towards hydrolysis. Through post-polymerization modification based on amine-reactivity, polymers containing PFP esters such as poly(pentafluorophenyl acrylates and methacrylates) have found interesting applications as useful reactive polymeric precursors due to easy functionalization with amine-containing moieties. Theato and coworkers developed the reactive polymers with facile synthesis for the post-polymerization modification based on pentafluorophenyl (PFP) esters which allows for convenient and versatile functionalization of (co)polymers and thin films with an excess of primary amines at room temperature with quantitative conversions in less than 1 h.[18-21]

In this part, we present poly(PFPA) brushes grafted on silica particles. As mentioned above, reactive polymer brushes were prepared by SI-RAFT polymerization and grafted onto the surface of silica particles to expand the surface area for applications. The prepared free polymers in solution were isolated and characterized by NMR, and GPC to monitor conversion, molecular weights. Successful synthesis of polymer brushes was characterized by TEM, TGA and XPS measurements. Based on the efforts within previous studies in our group to utilize PFP ester containing polymers as reactive polymer brush platforms, we envisioned that poly(PFPA)-based platforms may be an interesting material for diverse applications.

3.2. Experimental Section

Materials. Pentafluorophenol was purchased from Alfa Aesar (Ward Hill, MA, USA). Acryloyl chloride, triethylamine, and other solvents were purchased from Sigma Aldrich (St. Louise, Missouri, USA). Pentafluorophenyl acrylate (PFPA), used as the monomer, and benzyl dithiobenzoate (BDB), used as the RAFT chain transfer agent, was synthesized according to a method published before.[22] 2,2'-azobis(2-methylpropionitrile) (AIBN) was purified by recrystallization from methanol. Silica particles (0.255 μm, 1 μm, SD = 0.01 μm) in aqueous suspensions were obtained from Microparticles Gmbh (Berlin, Germany). Silica gel for column chromatography was purchased from Merck Chemical Company (Darmstadt, Germany).

Characterization. ^{1}H NMR spectra and ^{19}F NMR spectra were recorded on a Bruker Avance 500 MHz FT-NMR spectrometer (Bruker, Billerica, MA, USA). Chemical shifts were given in ppm relative to trimethylsilane. Gel permeation chromatography (GPC) was used to determine the molecular weight and the corresponding polydispersity index (PDI = M_w/M_n) of the polymer samples. GPC (YL9100, Young Lin Instrument Co. LTD.) measurements were performed under poly(styrene) standards in THF with 5 mg/mL polymer sample concentration. The modified silica particles were characterized with a Q500 thermogravimetric analyzer (TGA) (Q500, TA Instruments) and a transmission electron microscope (TEM) (JEM1010, JEOL)

with an acceleration voltage of 80 kV. The TGA sample was heated from room temperature to 700°C at a heating rate of 10°C/min under nitrogen flow (60 mL/min). The surface composition of SI-CTA-grafted SiPs, and functionalized and non-functionalized poly(PFPA)-grafted SiPs were also measured by X-ray photoelectron spectroscopy (XPS, AXIS-His, KRATOS), equipped with A1 monocromator anode and 18 mA / 12 kV X-ray power.

Synthesis of Dithiobenzoic Acid Benzyl-(4-ethyltrimethoxysilyl) Ester (SI-CTA). Dithiobenzoic acid benzyl-(4-ethyltrimethoxylsilyl) ester (SI-CTA) was synthesized following literature procedures.30 (Yield 17.3 g, 70%) 1H NMR (CDCl3) d: 7.98 (m, 1H), 7.27 (m, 8H), 4.54 (d, 2H), 3.54 (s, 9H), 2.73 (m, 2H), 1.02 (m, 2H). 13C NMR (CDCl3) d (ppm): 144.61, 134.81, 128.54,128.04, 50.38, 28.35, 11.09. FD mass spectra: 392.3 (100.0%), 3 93.3 (26.1%), 394.3 (12.4%), 274.2 (11.8%).

Immobilization of SI-CTA on Silica Particles. The dithiobenzoic acid benzyl-(4-ethyltrimethoxylsilyl) ester, used as the SI-RAFT chain transfer agent (SI-CTA), was synthesized following literature procedures. Modification of SI-CTA on SiPs was performed through silane coupling reaction. 1.20 mL (60.0 mg) of SiPs in aqueous suspension were repeatedly washed with ethanol, tetrahydrofuran (THF), and toluene, and separated by centrifugation. The recovered SiPs were then redispersed in 4 mL anhydrous toluene in a Schlenk flask. 0.030 g of SI-CTA dissolved in 3.5 mL anhydrous toluene were then added to the flask. The solution was stirred at 80

°C in an oil bath for 18 h. The modified SiPs were washed with toluene and dried in a vacuum oven at 80 °C overnight.

Synthesis of Poly(PFPA) Brushes on Silica Particles via SI-RAFT Polymerization. SI-CTA modified SiPs (53.2 mg) were dispersed in anhydrous anisole. The dispersed particles were then charged into a Schlenk flask, along with 5 mg (0.0205 mmol) of BDB, 0.4 mg (0.00244 mmol) of AIBN, and 2.24 g (9.41 mmol) of PFPA. After three freeze-pump-thaw cycles, the flask was backfilled with nitrogen, then stirred in an oil bath at 70 °C for 43 h. The polymerization was terminated by cooling the reaction to room temperature. The poly(PFPA)-grafted SiPs were rinsed with toluene and THF, then dried in a vacuum oven.

3.3. Results and Discussion

3.3.1. Surface-Initiated RAFT Polymerization of Poly(PFPA) Brushes

Dithiobenzoic acid benzyl-(4-ethyltrimethoxylsilyl) ester was first synthesized to enable the direct SI-RAFT from Si particles. For the immobilization of SI-CTAs, the silica particles in aqueous suspension was cleaned by toluene and Si-OH groups on surface of particles are used for the siloxane coupling of the thioester functional silanes. The particles were then immersed in toluene solution of S-CTA at 80 ℃ overnight to have OH groups of the substrate react with the methoxysilane groups from S-CTA. Afterward, heat treatment at 80 ℃ was performed overnight to achieve stable covalent bonds between the RAFT agent and the substrate. The modified surface was characterized by TGA (Figure 14), and when compared to bare SiPs, the presence of material grafted to SiPs was confirmed. Additionally, XPS measurements were conducted and peaks associated with C-S and C=S bonds of 2s sulfur originated from the dithioester groups on SI-CTA were observed (Figure 16).

Synthesis of poly(PFPA) brushes on SI-CTA-grafted SiPs was then carried out using SI-RAFT polymerization. The polymer brush molecular weight was estimated from the molecular weight of free poly(PFPA) chains generated using sacrificial free chain transfer agent, BDB, added to the polymerization mixture. It has been reported that the polymer brush molecular weight is actually comparable or smaller than the molecular weight of the bulk polymerized homopolymer.[23-24] However, the method is still useful in providing an upper limit estimation on brush

molecular weight. The particular poly(PFPA) brush was estimated to have a molecular weight of 40 kg/mol (PDI = 1.3). The presence of poly(PFPA) brushes on SiPs was further confirmed by TGA (Figure 14). By comparing the weight loss curve of polymer brushes to that of SI-CTA-grafted SiPs, the weight percent of poly(PFPA) brush relative to the total mass of poly(PFPA)-grafted SiPs was estimated to be 12.44 wt%. The polymer brushes can also be visualized by TEM. As shown in Figure 15, SiPs appear as dark spheres, surrounded by polymer brush shown with a lighter contrast. To further confirm that the polymer observed is a result of SI-RAFT polymerization, XPS data for polymer brushes were obtained and compared to those of SI-CTA-grafted SiPs (Figure 16). Following polymerization, S2p peaks associated with SI-CTA decreased while F1s peaks associated with PFPA units appeared, confirming that the polymer brush was indeed synthesized from the SI-CTA units attached on SiPs.

After polymerization, the particles became dissolved better in toluene and tetrahydrofuran. Pentafluorophenyl groups form unique low energy surfaces so poly(PFPA) brush-coated particles hardly dispersed in aqueous solution. For bioapplications which usually are applied in aqueous solution, post-polymerization modification of poly(PFPA) platforms is required.

Figure 13 Schematic on synthesis of Poly(PFPA) brushes on surface of silica particles via surface-initiated RAFT polymerization.

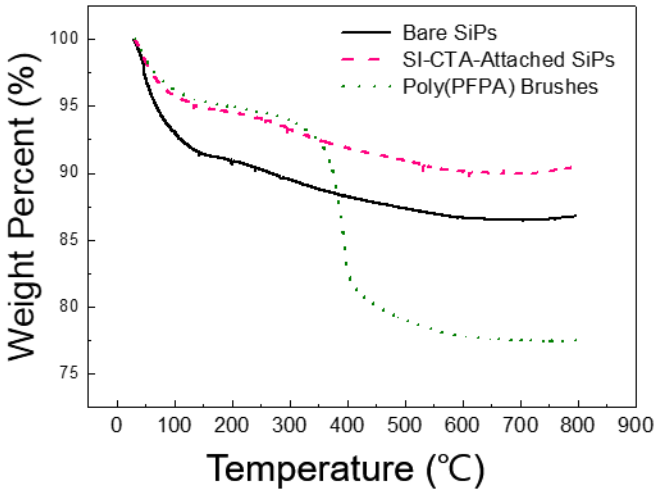

Figure 14 TGA curves of bare silica particles, surface-initiated RAFT chain transfer agent (CTA)-attached and poly(PFPA) brush-coated particles.

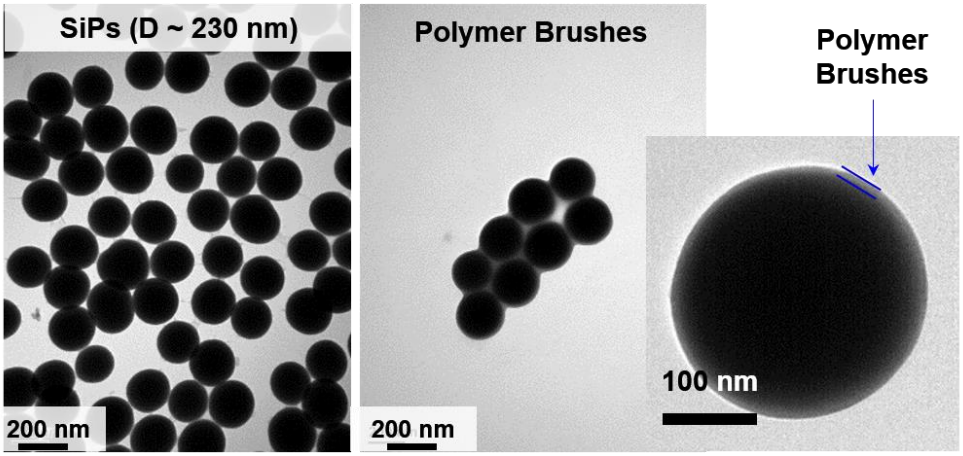

Figure 15 TEM images of bare silica particles and polymer brush-coated particles.

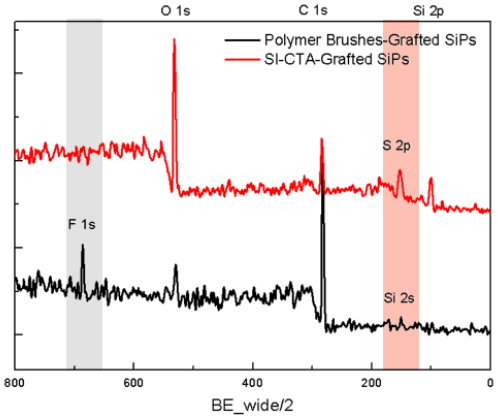

	Atomic Conc. %	
	Polymer Brushes	SI- RAFT CTA
Si 2p	5	33.99
S 2p	0	4.04
C 1s	76.42	24.15
O 1s	10.66	37.82
F 1s	7.92	0

Figure 16 XPS curves and the table of atomic concentration % shows S 2p peak originated from SI-CTA-attached silica particles and F 1s peak in polymer brush-coated silica particles.

3.3.2. Polymerization of Polymer Brushes in Different Molecular Weights

We then synthesized poly(PFPA) brushes with different molecular weights and saw the difference in dispersion of particles in aqueous solution. Relatively low (12,250 g/mol; PDI 1.16), medium (32,537 g/mol; PDI 1.27), and high (71,715 g/mol; PDI 1.32) molecular weight of polymer brushes were prepared by Si-RAFT polymerization on same silica particles. The brush molecular weight was estimated based on the free poly(PFPA) homopolymer synthesized from sacrificial BDB. The weight percent of poly(PFPA) relative to the total mass of poly(PFPA)-grafted SiPs was calculated using TGA weight loss measurement.

Figure 17 shows the differences in weight losses polymer brush-coated particles with low, medium, and higher molecular weight of poly(PFPA) compared to that of SI-CTA-attached silica particles. By subtracting weight loss in SI-CTA-coated particles, the weight percentage of poly(PFPA) brushes in the samples are 6. 86 %, 11.82 % and 16.89 % relative to the total amount of poly(PFPA) brush-grafted particles. Particularly low molecular weight of poly(PFPA)-grafted silica particles show remarkably better dispersion in water. In aqueous solution, non-modified poly(PFPA) brushes with longer chains have collapsed conformation and brush-grafted particles tend to be aggregated more to reduce surface area exposed to water. Solvent molecules in aqueous solution have a strong affinity for the silica particles on which the polymer chains are grafted and relatively more chances to penetrate

solvent molecules into lower molecular weight polymer brush layer on the surface of silica particles.[25-26]

To test the high reactivity of reactive polymer brushes based on activated esters, the facile introduction of amine containing fluorescent dye molecules like 5- ((2-aminoethyl) amino) naphthalene-1-sulfonic acid (EDANS) was performed. Our group has previously reported that EDANS dyes are the relevant compounds showing both high conversion with PFP-ester functional groups and the efficient fluorescence characteristic.[27] Accordingly, 1 mg of polymer brush-coated particles was treated and shaken for 1 h at room temperature in 2 mL of DMSO solution containing 20 mg of EDANS. Afterward, the particles were centrifuged and washed several times with DMSO. As shown in Figure 19, the blue fluorescence originating from the EDANS molecules (λ_{ex} = 365 nm and λ_{em} = 490 nm) was demonstrated from photoluminescence experiments, which were covalently bound to polymer brushes. Lower (25 kg/mol) and higher (50 kg/mol) molecular weight of polymer brushes were treated in same concentration of EDANS solution, which showed different intensities. This experiment clearly demonstrates the novel and easy approach toward the precise post-modification of reactive polymer brushes that allow the subsequent functionalization resulting in changes of whole polymer brushes in chemical properties.

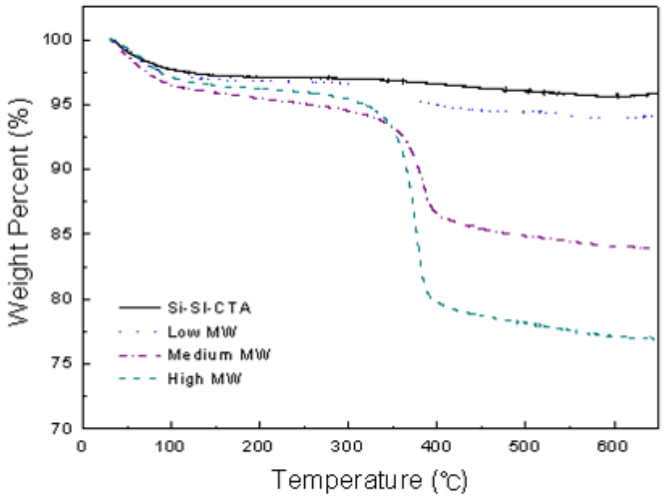

Figure 17 TGA curves of poly(PFPA) brush-coated silica particles with three different molecular weight (12, 33, 72 kg/mol). Compared with the curve of SI-CTA-attached particles, the weight percentage of poly(PFPA) brushes in the three samples are calculated as 6.86%, 11.82 %, and 16.89 %, respectively.

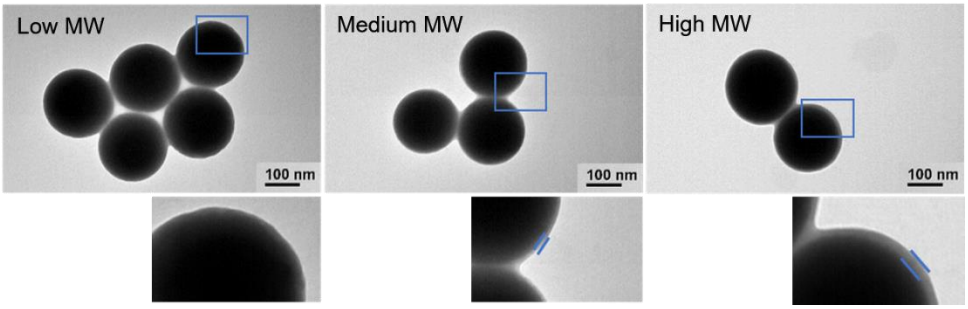

Figure 18 TEM images of polymer brush-grafted silica particles in different molecular weights such as low, medium and high molecular weight.

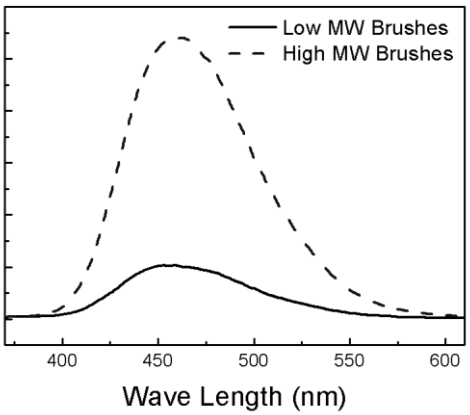

Figure 19 Photoluminescence data of poly(PFPA) brush-coated silica particles with two different molecular weight (25 and 50 kg/mol) after post-polymerization modification. The blue fluorescence was originated from the EDANS dye molecules.

3.3.3. Grafting Density of Polymer Brushes on SiPs

We synthesized poly(PFPA) brushes with different molecular weights as well as with different size of SiPs (1 μm). The polymer brush was successfully grafted on the silica particles with molecular weight (70, 100 kg/mol) and characterized by TEM images and TGA curves (Figure 20-21).

In case of flat surface, the grafting density of polymer brushes were calculated using the thickness of the graft and the density of polymer repeat unit. But, in case of brush on spherical surface, Grafting density (σ_{TGA}) was usually calculated like below using the weight % of poly(PFPA) and SiPs from TGA curves, radius of SiPs (r_{SiPs}) and density of bare silica particles (ρ_{SiPs} = 1.05 g/cm^3).[28]

$$\sigma_{TGA} = \frac{\frac{wt\%_{PPFPA}}{wt\%_{SiPs}} \rho_{SiPs} \frac{4}{3} \pi r_{SiPs}^3 N_A}{M_n 4\pi r_{SiPs}^2}$$

The grafting density of poly(PFPA) brush particles were near 0.08 chains/nm2 and slightly changed depending on the molecular weight of brushes and the amount of surface-initiated CTA used. Table 1 demonstrates that poly(PFPA) brushes have been successfully grafted and exists on the silica surface as somewhere near semi-dilute brushes.

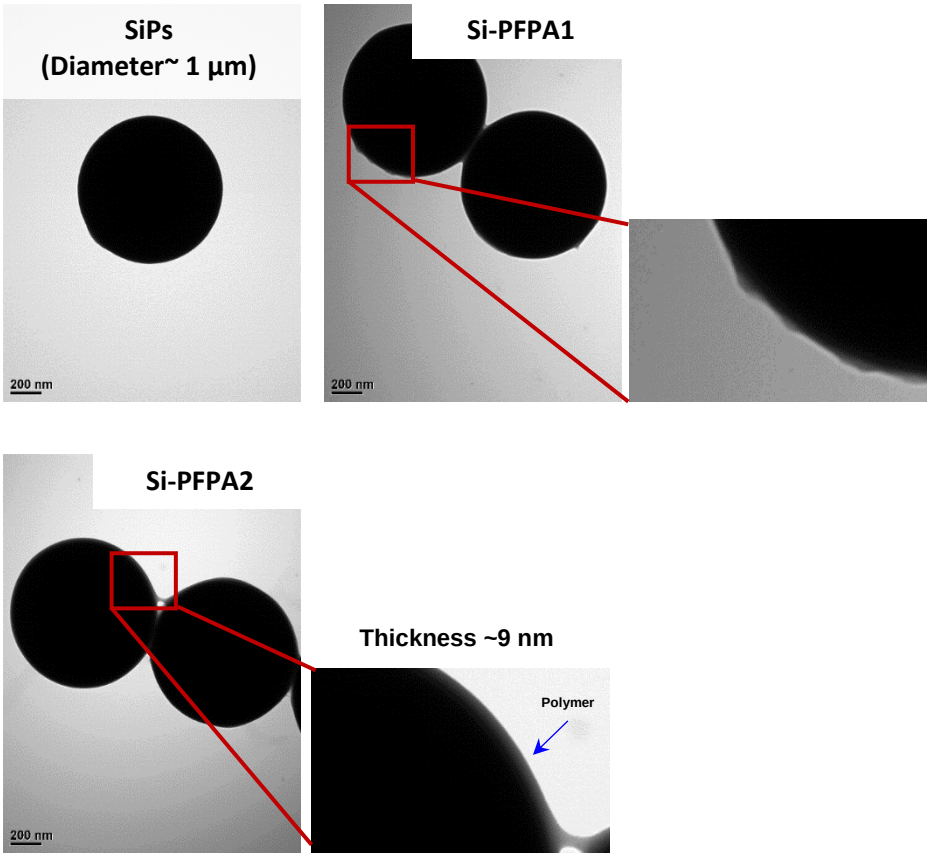

Figure 20 TEM images of poly(PFPA) brushes on SiPs (diameter 1000 nm) with different molecular weight. (70, 100 kg/mol)

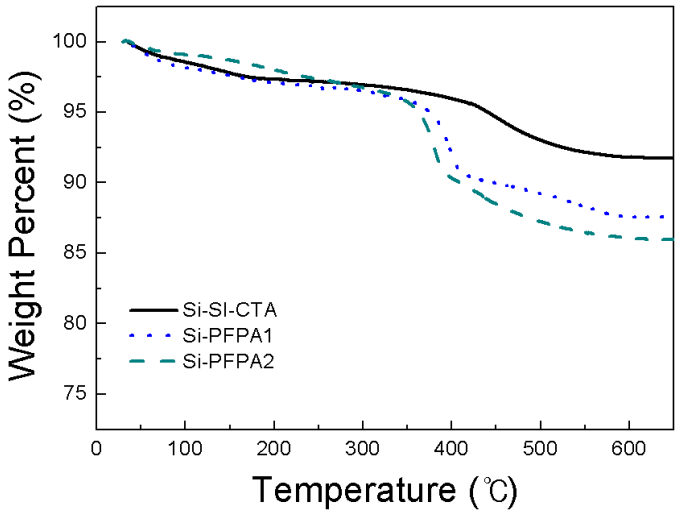

Figure 21 TGA curves of SI-CTA-attached and poly(PFPA) brush-grafted SiPs.

Diameter (nm)	M_n (g/mol)	Weight % of PPFPA (%)	Weight % of SiPs (%)	σ, Grafting Density (chains/nm^2)
250	32537	11.9	83.9	0.08
250	71715	18.9	77.0	0.07
1000	70645	4.5	85.9	0.10
1000	99259	5.8	87.6	0.08

Table 1 Molecular weight (M_n) and the calculated grafting density of poly(PFPA) brushes on SiPs based on weight percent from TGA data.

3.4. Conclusion

Reactive polymer brushes, based on PFP acrylate monomers, have been prepared using the surface reversible addition and fragmentation chain transfer polymerization strategy. The surface coverage controlled by the increase in molecular weight of polymer brushes. We further demonstrated that the activated ester moieties remaining in the reactive polymer brushes could be used for post modification, yielding fluorescent surfaces. It demonstrated the versatility of the activated polymer brushes approach, which combines both the precise control of S-RAFT polymerization and the easy post modification to virtually any functionality to create functional films in response to desired demands. We believe that our platform will open new strategy to prepare functional polymer brushes without difficult synthesis and modification step to applied biological application.

Chapter 4. Reactive Polymer Brush-Grafted Particles for Immunoprecipitation

4.1. Introduction

Immunoprecipitation (IP) experiments[1-3] are one of such bioapplications, which was first developed as a small-scale affinity purification with the purpose of an adaptation of column affinity chromatography. It is routinely performed by biologists to isolate specific antigens and to identify their interactors from complex protein mixtures for the purpose of subsequent detection. The basic form of IP tools, commercially available, is antibody-bound solid support such as agarose resin or magnetic particles to capture and separate specific targeting protein complexes. The conventional approach involving agarose supports utilizes protein A or G which selectively binds to the heavy chain within the Fc region of most antibodies for good antibody-binding capability. Agarose-based IP, however, often suffers from strong nonspecific binding and antibody contamination, resulting in high background as shown in the results of electrophoresis.

To get the clear results after IP experiments, other immobilization kit using crosslinker between antibody and protein A/G was developed, but even this system

uses agarose support and is not free from problems caused by strong nonspecific binding. Moreover, the use of amine-reactive activated esters[4-6] such as N-hydroxysuccinimidyl, or NHS, esters, which typically used for crosslinking with amine-containing biomolecules, for covalent immobilization has also been studied. However, long reaction time is required due to relatively lower reactivity and poor hydrolytic stability of NHS esters.

Recently, a new type of activated ester, the pentafluorophenyl, or PFP ester, is receiving attention due to its high reactivity with amines along with their enhanced resistance towards hydrolysis. Through post-polymerization modification based on amine-reactivity, polymers containing PFP esters such as poly(pentafluorophenyl acrylates and methacrylates) have found interesting applications as useful reactive polymeric precursors due to easy functionalization with amine-containing moieties. Particularly, those functional polymers demonstrate the possibility in a range of applications in the form of polymer brush[7-10], which is more stable because one end of each polymer chain is tethered on a substrate. Based on the efforts within previous studies in our group to utilize PFP ester containing polymers as reactive polymer brush platforms, we envisioned that poly(pentafluorophenyl acrylate), or poly(PFPA), may be an interesting material for IP applications..

In this paper, we introduce a biomolecule-immobilized polymer brush as a platform for IP based on the amine-reactivity of poly(PFPA). Reactive polymer brushes are grafted on the surface of silica particles[11-14] via SI-RAFT polymerization. Amine-containing biomolecules such as antibodies and other functional molecules

easily reacted with poly(PFPA) brush-coated particles, and consequently the efficiency of polymer brush platforms applied to IP was controlled by the degree of modification with amino-terminated PEG as well as molecular weight of poly(PFPA) brushes. To reduce the antibody contamination and nonspecific protein after purification, we present IP experiments using poly(PFPA) brush-coated particles to make antibodies immobilized stably by covalent bonding and prevent nonspecific binding. The proteins bound within brush shell can be released by changing the environmental conditions, such as pH and ionic strength of the system and detected by western blotting and other assay techniques. In order to enhance the capture efficiency of antibodies, the optimized condition of on and poly(PFPA) brush grafted on particles was found after the study on the effect of post-treatment with amino-terminated PEGs.[15] Based on these studies, poly(PFPA) brush-based platforms would be further extended into diverse biomolecule immobilization applications.

4.2. Experimental Section

Materials. All the chemicals and other solvents were purchased from Sigma Aldrich (St. Louise, Missouri, USA). Silica particles (0.255 μm, SD = 0.01 μm) in aqueous suspensions were obtained from Microparticles Gmbh (Berlin, Germany). ω-Amino Terminated poly(ethylene glycol) methyl ether (Mn = 550 g/mol, PDI = 1.15) with was purchased from Polymer Source, Inc. (Dorval, Québec, Canada). PKR (D7F7) Rabbit mAb (74 kDa) purchased from Cell Signaling Technology, Inc. (Danvers, MA, USA) was used for the IP test. TRBP antibody was purchased from AbFrontier and GAPDH antibody was purchased from Santa Cruz Biotechnology.

Characterization. The modified silica particles were characterized with a Q500 thermogravimetric analyzer (TGA) (Q500, TA Instruments) and a transmission electron microscope (TEM) (JEM1010, JEOL) with an acceleration voltage of 80 kV. The TGA sample was heated from room temperature to 700°C at a heating rate of 10°C/min under nitrogen flow (60 mL/min). The surfaces of functionalized poly(PFPA) brush on both silicon wafer and SiPs were examined in attenuated total reflectance (ATR) mode by Fourier transform infrared spectroscopy (FT-IR, TENSOR27, Bruker). The surface composition of functionalized and non-functionalized poly(PFPA)-grafted SiPs were also measured by X-ray photoelectron spectroscopy (XPS, AXIS-His, KRATOS), equipped with A1 monocromator anode and 18 mA / 12 kV X-ray power. The dispersion of the PEG-grafted polymer brush

silica particles in water was compared by the dynamic light scattering (DLS) measurement using zetasizer nano zs90 (Malvern Instruments).

Synthesis of Poly(PFPA) Brushes on Silica Particles via SI-RAFT Polymerization. SI-CTA-modified particles (53.2 mg) were dispersed in anisole. The dispersed particles and the solution of 5 mg (0.0205 mol) of BDB and 0.4 mg (0.00244 mmol) of AIBN were placed into a Schlenk flask, and 2.24 g (9.41 mmol) of PFPA was added to the solution. After three freeze-pump-thaw cycles were performed, the flask filled with nitrogen gas was stirred in an oil bath at 70 ℃ for 43 h and cooled down to the room temperature. The polymer-grafted particles were rinsed with toluene and THF several times and dried in a vacuum oven.

Post-Treatment with Amine-Terminated Poly(ethylene glycol) (PEG). Amine-terminated PEG dissolved in THF (0.5 ml) were added into the suspension of polymer brush-grafted particles in 0.5 ml THF and then the reaction mixtures were stirred for 16 h at room temperature. After the reaction, the PEG-substituted polymer brushes were washed with THF several times and dried in vacuum.

Immunoprecipitation (IP). The first step of IP using poly(PFPA) brush-coated silica particles is crosslinking of antibodies. Antibody immobilization was performed on either silicon wafers or silica particles grafted with poly(PFPA) brushes. In both scenarios, the substrate material was placed in a desired solvent

containing 5 μg of PKR antibodies. The mixture was incubated with rotation at 4 ℃ overnight.

HeLa cell pellets were suspended in Tris-based lysis buffer (50 mM Tris-HCl pH 8.0, 100 mM KCl, 0.5% NP-40, 10% Glycerol, 1mM DTT) supplemented with protease inhibitor cocktail (Calbiochem) and incubated on ice for 10 min. Cells were then sonicated using Bioruptor and debris was separated by centrifugation. Lysates were then incubated with antibody-conjugated SiPs for 3 h at 4 ℃. SiPs were washed 3 times with the lysis buffer and SDS loading buffer was added to elute the proteins attached to the antibody on the bead surface. Eluted protein was heated to 95 ℃ for 10 min and was subjected to further analysis using gel electrophoresis.

Target antigen used in this paper is protein kinase R (PKR). TAR RNA-binding protein (TRBP) is also separated. The nonspecific protein, glyceraldehyde 3-phosphate dehydrogenase (GAPDH), is used for a negative control.

4.3. Results and Discussion

4.3.1. Post-Treatment of Polymer Brushes with Amino-Terminated PEGs

Instead of traditional agarose-based beads for IP, poly(PFPA) brush-coated particles were used to separate target protein from protein mixture. The amine-reactive functional groups of these polymer brush possesses a good leaving group that can undergo nucleophilic substitution to form an amide bond with primary amines in biomolecules. PKR antibodies were first attached to poly(PFPA) brush-coated particles by covalent immobilization of active ester-amine chemistry and antibody-attached particles were dipped into protein mixtures. Then PKR, target protein, was bound to PKR antibodies existed on poly(PFPA) brush particles by specific antigen-antibody binding and lots of other nonspecific proteins could be reacted with the remained pentafluorophenyl groups in poly(PFPA) chains.

Following the successful synthesis of poly(PFPA)-grafted SiPs, antibody was immobilized on the particle surfaces by incubation of polymer-grafted SiPs with antibody in a suitable solvent. Two different solvents, PBS and DMSO, were tested for antibody immobilization. PBS is the typical solvent used when dealing with biomacromolecules. However, poly(PFPA)-grafted SiPs are not well-dispersed in aqueous solution due to low surface energy, thus DMSO is chosen as an alternative solvent to improve SiPs dispersion.

The antibody immobilized SiPs, prepared in either PBS or DMSO, were used

in IP experiments. In a typical setup, antibody immobilized SiPs are added to cell lysate containing total protein extracted from cells. The mixture is shaken to allow antibody-protein binding, and the bound target protein is then pulled-down along with the SiPs via centrifugation. The proteins are then separated from the solid substrate using an elution buffer and analyzed by gel electrophoresis.

For the initial experiments, anti-PKR antibody was immobilized on poly(PFPA) brushes. Following IP, silver staining was used to visualize all proteins isolated with SiPs. Figure 22 shows silver staining results for proteins immuoprecipitated using poly(PFPA)-grafted SiPs conjugated with antibody, as well as ones recovered using commercially available Protein A based IP kit. The most noticeable difference is the amount of proteins recovered via the two different methods. When Protein A based traditional IP is used, a large number of non-target proteins are recovered in addition to the target. Since Protein A is an efficient protein binder, it is known to interact non-specifically with a number of different proteins, leading to a high background. In comparison, when IP is performed using poly(PFPA)-grafted SiPs conjugated with antibody, the number of non-target proteins recovered is significant less, resulting in a much cleaner protein separation. Another observation we can make from the silver staining results is that protein bands located at ~55 kDa and ~27 kDa are present in significant concentration in conventional IP recovered sample, but almost completely absent in poly(PFPA)-based IP scheme. These bands correspond to the heavy and light chains of the antibody, respectively. A major short-coming of Protein A/G based IP is that during

protein elution, both the bound proteins and the immobilized antibody are eluted. Therefore, the solid substrate loses its antibody after just one use. More importantly, the presence of eluted antibody complicates data interpretation. If the target protein also eludes near 55 kDa or 27 kDa, then to distinguish the target from the antibody is almost impossible. For the poly(PFPA) based IP scheme, antibody is immobilized by covalent bond, thus they are not eluted during protein recovery, as confirmed by silver staining results. Consequently, the spectrum of the recovered protein is not complicated by extra bands from the immobilized antibody. Furthermore, with proper washing, the antibody bound SiPs can potentially be reused for multiple IPs.

To determine the efficiency of target protein recovery, the eluted protein sample was further analyzed via western blotting. Three different antibodies were used for examination: anti-PKR antibody was used to visualize the amount of PKR (target protein) immunoprecipitated; anti-TRBP antibody was used to visualize protein TRBP, a known interactor with PKR, thus co-immunoprecipitate with PKR; and anti-GAPDH antibody was used as a negative control as GAPDH is an abundant protein that does not interact with PKR. Figure 23a shows the western blot data of protein samples recovery using antibody-bound SiPs prepared in either PBS or DMSO solvent. When PBS is used as the solvent for antibody immobilization, despite the poor dispersion of SiPs, PKR enrichment is observed as indicated by the presence of PKR band and absence of GAPDH band. Furthermore, weak TRBP band is also seen, indicating that the degree of PKR enrichment is high enough such that

its interactor protein can also be co-purified. Surprisingly, when the IP experiment is conducted using antibody immobilized SiPs prepared in DMSO, no protein bands are observed. Despite the improved particle dispersion, we conclude that DMSO is not a suitable solvent for antibody immobilization.

However, the intensity of band of PKR was low due to the antibody orientation on surfaces of polymer brushes. Pentafluorophenyl groups in poly(PFPA) brushes react randomly with primary amines (-NH2) which exist at the N-terminus of each polypeptide chain and in the side chain of lysine (Lys, K) amino acid residues. Contrary to the bioaffinity immobilization of antibodies to support using protein A/G, covalent bonding between polymer brushes and antibodies could block the binding site in antibodies because primary amine groups are abundant and distributed over the entire antibodies. Number of functional groups in polymer chains increase opportunities for antibodies to be attached with polymer brushes and that complement the attachment of randomly-oriented antibodies. Moreover, poly(PFPA) brushes surrounding silica particles lead to the collapsed conformation of polymer chains in aqueous solution due to the hydrophobicity of poly(PFPA). Pentafluorophenyl groups form unique low energy surfaces so poly(PFPA) brush-coated particles hardly dispersed in aqueous solution such as PBS solution for attachment of antibodies.

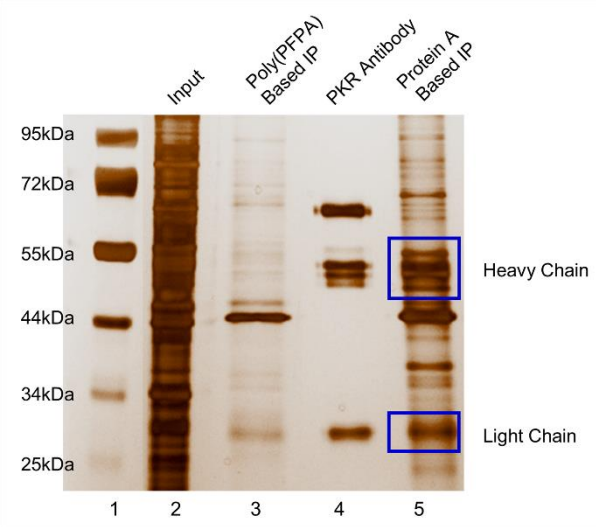

Figure 22 Silver staining results for proteins immunoprecipitated using poly(PFPA) based IP (lane 3) and conventional Protein A based IP kit (lane 5). Lane 1 shows the protein ladder. Lane 2 shows the input protein mixture before IP. Lane 4 shows the anti-PKR antibody immobilized on poly(PFPA) brush. The blue boxes indicate heavy and light chains of anti-PKR antibody.

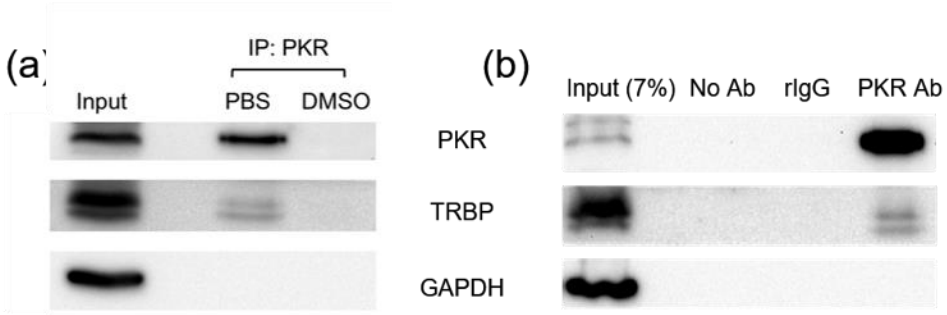

Figure 23 Western blot images of (a) polymer brush-coated particles using PKR antibodies and of (b) polymer brush-coated particles after the treatment with 10 % amino-terminated PEG solution. PKR is the target protein and TRBP is the protein that forms complexes with PKR. The negative control, GAPDH is the nonspecific protein. Polymer brush particles without incubation in PKR antibodies and polymer brush particles after incubation in rabbit IgG (rIgG) antibodies were also used for the negative control.

To improve the efficiency of poly(PFPA)-grafted SiPs for IP applications, overcoming particle hydrophobicity is critical, especially since conducting antibody immobilization in organic solvent is shown to be not feasible. The PFP groups form unique low energy surfaces so poly(PFPA) brushes are not well solvated in water. The polymer brushes have collapsed conformation, which means antibody molecules cannot penetrate deep into the brushes to react with PFP units. In addition, the poly(PFPA)-grafted SiPs aggregate in aqueous solvent to reduce exposed surface area, further reducing the number of exposed PFP units available for reaction.

We attempted to change the surface property of poly(PFPA)-grafted SiPs by grafting small hydrophilic polymer chains to the polymer brushes. In particular, low molecular weight (Mn = 550 g/mol, PDI = 1.15) amino-terminated PEG polymers were used for this purpose. Since these PEG polymers contain amine functionality at the chain end, they can be grafted to poly(PFPA) using the same PFP ester-amine reaction used for antibody attachment. The PEG treatment would necessarily reduce the number of PFP units available for further antibody immobilization; however, we hypothesize that by controlling the number of PEG substitution sites, the poly(PFPA) brush can still retain sufficient number of free PFP units for antibody attachment while significantly improving its surface hydrophilicity. Additionally, PEG is known for its ability to repel non-specific protein binding, so its presence may further reduce background noise of our IP design. The modified poly(PFPA) brush particles were characterized by XPS and IR to confirm the immobilization of amine-containing molecules. (Figure 24-25)

To prepare PEG-substituted poly(PFPA) brushes, the poly(PFPA)-grafted SiPs were combined with amino-PEG in THF. Assuming every PFP unit react immediately with every amine end group of amino-PEG, different concentrations of PEG solutions were prepared to yield 10%, 50%, and 100% theoretical substitution of PEG relative to the total number of available PFP units on polymer brushes. The silica particles thus prepared are labelled x % PEG-substituted SiPs, where x represents the theoretical degree of PEG substitution. The PEG-substituted SiPs were then dispersed in water, and their particle size information were measured by DLS. The dispersion properties of poly(PFPA)-grafted SiPs with different degrees of theoretical PEG substitution are summarized in Figure 26. The non-substituted poly(PFPA)-grafted SiPs do not disperse well in water and the particles appear as large aggregates. As the degree of PEG substitution increases, particle dispersion is seen to improve significantly as the solution turns into a misty suspension. The hydrodynamic diameters of the particles are measured by DLS, and the Z-average values are reported. As the percent PEG substitution increases, particle size also increases. Since the silica core cannot expand, the increase in particle size suggests that the polymer brushes surrounding the silica particles are becoming more solvated thus more swollen in water. Note that for the 0% and 10% PEG-substituted SiPs, partial aggregation was observed, so the reported Z-average values were determined based on the non-aggregated population of SiPs.

According to our hypothesis, a swollen poly(PFPA) brush conformation would increase the efficiency of antibody attachment, in comparison to a collapsed

conformation, as the swollen brushes would allow a larger number of PFP units to be exposed for reaction. To test the hypothesis, the 10% PEG-substituted SiPs were used in an IP experiment, again having anti-PKR as the immobilized antibody. Figure 23b shows the western blot data for immunoprecipitated PKR, TRBP, and GAPDH. Selective enrichment of the target PKR over non-target GAPDH is observed, along with the successful co-precipitation of the PKR-interactor, TRBP. Furthermore, when comparing the amount of PKR immunoprecipitated using 10% PEG-substituted SiPs with those recovered using non-PEG-treated SiPs (Figure 23a), a significant increase in IP efficiency was observed. This improvement can be mainly attributed to the increased number of immobilized antibody on 10% PEG-substituted SiPs. Although a theoretical 10% of the PFP sites are occupied by PEG, the improvement in surface hydrophilicity allows the poly(PFPA) brushes to swell sufficiently in an aqueous environment such that the net effect is an increased number of accessible PFP units for antibody reaction. We also speculate that with the particle surfaces being more hydrophilic, it may provide a friendlier environment for antibody-protein interaction, which can also lead to increased IP efficiency.

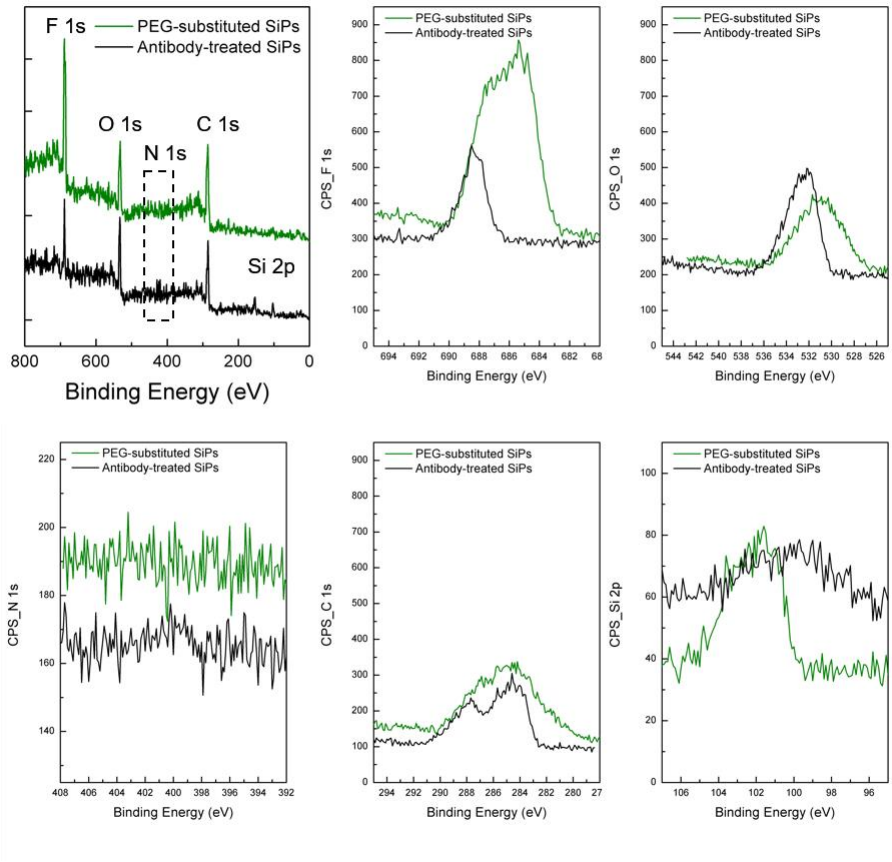

Figure 24 XPS data of poly(PFPA) brush grafted on SiPs after antibody incubation (black), and 10% PEG substitution reaction (green). Detailed spectra for F 1s, O 1s, N 1s, C 1s, and Si 2p peaks are demonstrated.

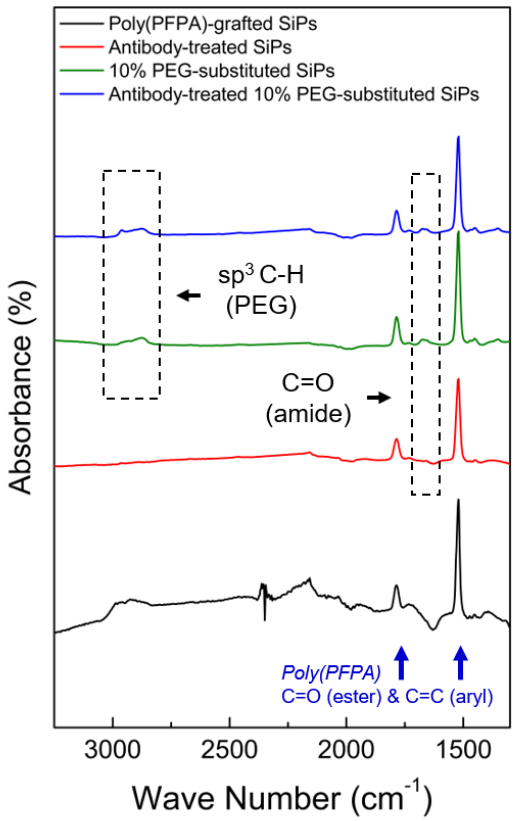

Figure 25 FT-IR data for untreated poly(PFPA)-grafted SiPs (black), and poly(PFPA)-grafted SiPs treated with antibody (red), 10% amine-PEG (green), and 10% amine-PEG then antibody (blue).

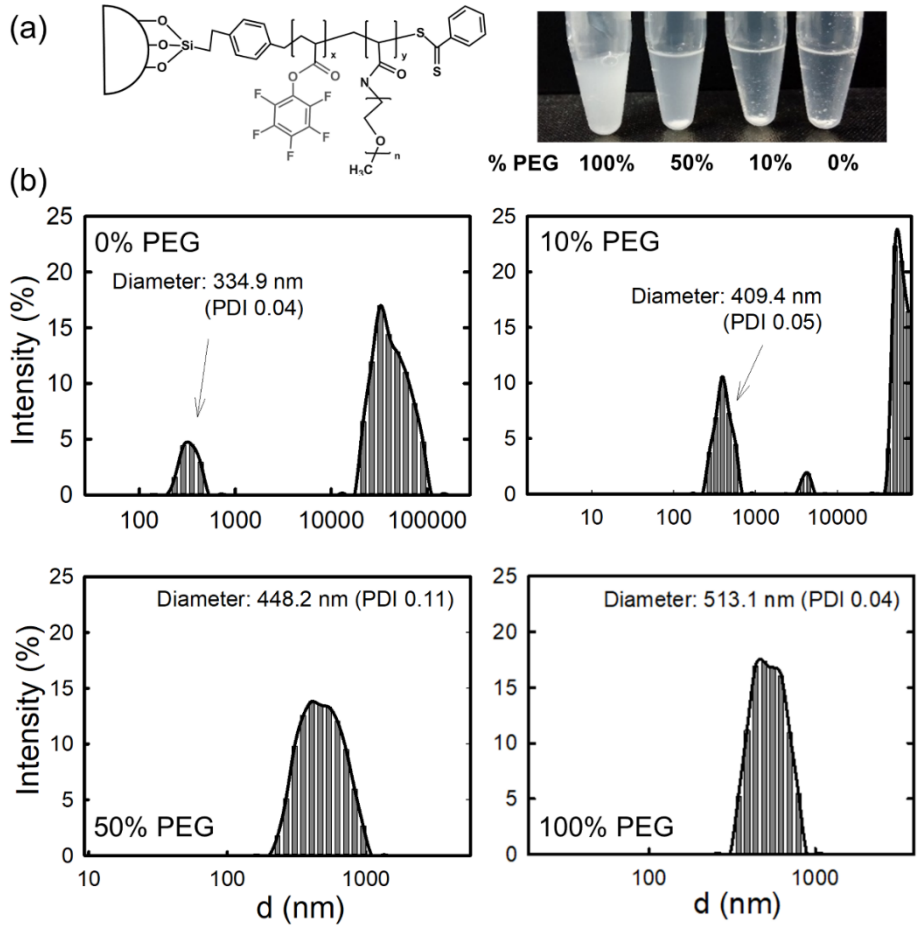

Figure 26 (a) Physical appearance of poly(PFPA)-grafted SiPs with different degrees of amino-PEG substitution when dispersed in water. (b) DLS measurements of poly(PFPA)-grafted SiPs with 0%, 10%, 50%, and 100% theoretical PEG substitution. The Z-average diameter and PDI of each sample are also reported. For the 0% and 10% PEG-substituted SiPs, partial aggregation is observed so the numbers reported are determined based on the peaks for non-aggregated particles only.

4.3.2. Molecular Weight Effect on the Poly(PFPA) Brushes Used for Immunoprecipitation

We then tested poly(PFPA) brushes with different molecular weights and saw the difference in dispersion of particles in aqueous solution. Relatively low (12 kg/mol), medium (33 kg/mol), and high (72 kg/mol) molecular weight of polymer brushes were prepared by Si-RAFT polymerization on same silica particles. Medium molecular weight of polymer brush-grafted silica particles was already used before to test the potentiality of poly(PFPA) brush particles for IP. As mentioned above, particularly low molecular weight of poly(PFPA)-grafted silica particles show remarkably better dispersion in water. In aqueous solution, non-modified poly(PFPA) brushes with longer chains have collapsed conformation and brush-grafted particles tend to be aggregated more to reduce surface area exposed to water. Solvent molecules in aqueous solution have a strong affinity for the silica particles on which the polymer chains are grafted and relatively more chances to penetrate solvent molecules into lower molecular weight polymer brush layer on the surface of silica particles.

The low-, medium-, and high-MW samples were each treated with PEG solution such that 10% theoretical PFP unit substitution was achieved. The PEG-substituted samples were then immobilized with anti-PKR antibody, and tested for IP performance. For comparison, PEG-substituted SiPs without antibody attachment were also prepared, and they were labelled as “blank” samples. Six separate IP

experiments involving poly(PFPA)-grafted SiPs of three different brush molecular weights were performed. The western blot data showing the amount of immunoprecipitated target protein (PKR) and the amount of non-target protein (GAPDH) from all six IP experiments are summarized in Figure 27. The blank samples, regardless of the poly(PFPA) brush molecular weight, show no noticeable protein recovery, indicating that the substrate material itself has minimal interaction with the protein mixture. For the low-, medium-, and high-MW brushes with antibody immobilized on the particle surface, selective concentration of the target protein over non-target protein is confirmed for all three brushes. In particular, the low- and medium-MW samples show stronger PKR band than the high-MW sample, indicating more efficient target protein recovery. Although the lower molecular weight brushes contain fewer number of PFP units, their better dispersion property in aqueous solution more than compensates for this deficiency, such that the total number of PFP units accessible for antibody reaction is higher in the lower molecular weight samples. This then leads to a larger number of immobilized antibody in the lower molecular weight brush samples, and consequently the better IP performance.

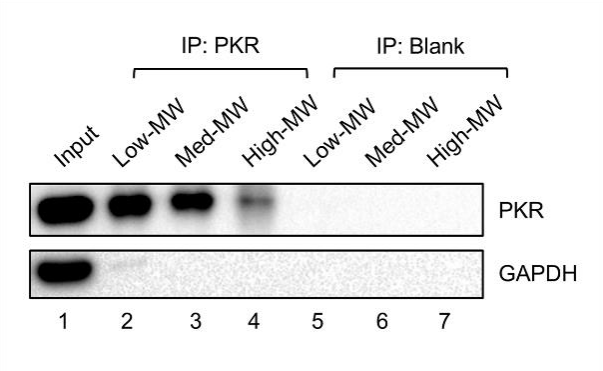

Figure 27 Western blot for proteins recovered from IP using poly(PFPA) brushes of different molecular weights. Lane 1: input protein mixture before IP. Lane 2: IP using low-MW poly(PFPA) brush, with 10% PEG-substitution, followed by anti-PKR antibody incubation. Lane 3: IP using medium-MW poly(PFPA) brush, with 10% PEG-substitution, followed by anti-PKR antibody incubation. Lane 4: IP using high-MW poly(PFPA) brush, with 10% PEG-substitution, followed by anti-PKR antibody incubation. Lane 5: IP using low-MW poly(PFPA) brush, with 10% PEG-substitution, no antibody treatment. Lane 6: IP using medium-MW poly(PFPA) brush, with 10% PEG-substitution, no antibody treatment. Lane 7: IP using high-MW poly(PFPA) brush, with 10% PEG-substitution, no antibody treatment.

4.3.3. Post-Modification of Poly(PFPA) Brush-Grafted Particles with Different PEG-Amines for Immunoprecipitation

Besides controlling poly(PFPA) brush molecular weight, the PEG treatment also plays an important role in determining IP performance. As demonstrated in earlier sections, when using the same poly(PFPA)-grafted SiPs, a 10% PEG substitution improves particle surface hydrophilicity and leads to significant improvement in IP efficiency. However, every site of PEG substitution means that the site is no longer available for subsequent antibody immobilization. There must exist a threshold, beyond which PEG substitution would lead to decreased IP performance.

Using the low-MW poly(PFPA) brushes, three different degrees of PEG substitution were examined: 1%, 10%, and 50%. The PEG-substituted SiPs were immobilized with anti-PKR antibody, then used for IP experiments. The resulting western blot data are shown in Figure 28. Selective enrichment of the target PKR protein is seen for all three samples with different degrees of PEG substitution. While the PKR band intensity is similar for 1% and 10% PEG-substituted SiPs, it's significantly weaker for 50% PEG-substituted SiPs. At 50% PEG substitution, too many PFP units are sacrificed for PEG attachment. Even though the polymer brush is well solvated in aqueous solution, there are not enough PFP units remaining for antibody reaction. Additionally, at high degree of PEG substitution, the density of PEG molecules on the particle surface is expected to be high. They might pose steric

hindrance and prevent antibody, which is fairly large in size (2 ~ 10 nm), to access the free PFP units remaining on the particle surface. At moderate degree of PEG substitution (~10%), the poly(PFPA) brushes are solvated, while the PEG layer is not too dense, thus allowing sufficient number of PFP units to be available for antibody reaction. We conclude that by reaching an optimal balance between surface hydrophilicity and number of accessible PFP units, efficient protein separation with reduced non-specific background can be achieved using poly(PFPA) based IP schemes.

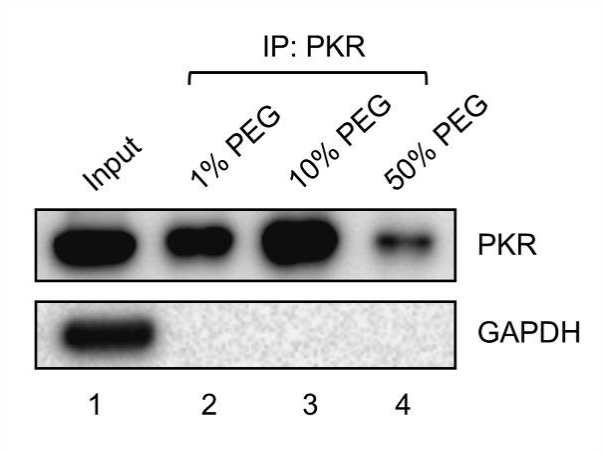

Figure 28 Western blot for proteins recovered from IP using low-MW poly(PFPA)-grafted SiPs treated with different amino-PEG substitution. Lane 1: input protein mixture before IP. Lane 2: IP using 1% PEG-substituted SiPs, followed by anti-PKR antibody incubation. Lane 3: IP using 10% PEG-substituted SiPs, followed by anti-PKR antibody incubation. Lane 4: IP using 50% PEG-substituted SiPs, followed by anti-PKR antibody incubation.

4.4. Conclusion

Poly(PFPA) brushes-coated silica particles were subject to post-modification with amine-containing biomolecules based on the fast reactivity with primary amines. Amine-reactive polymer brushes were grafted on silica particles via SI-RAFT polymerization and show the possibility of replacing traditional agarose-based IP kit with poly(PFPA) brush-based platforms. IP experiments were used for the isolation of specific protein from protein mixtures by antigen-antibody binding. Covalent bonds between antibodies and poly(PFPA) brushes surrounding silica particles result in no contamination of antibodies and nonspecific proteins in background data. However, the hydrophobicity of poly(PFPA) and the random oriented immobilization of antibodies affect the capture efficiency of target protein. Post-modification using more hydrophilic and protein-repellant PEG-amine was introduced to poly(PFPA) brush platforms so that polymer brush could be less collapsed in aqueous solution and subsequently antibodies of target antigen were attached. As a result, the modified poly(PFPA) brush-based particles demonstrates the better efficiency of IP. Furthermore, by changing molecular weight of poly(PFPA) brushes and the substituted percentage of PEG with PFPA, the optimized condition becomes clear that low molecular weight of poly(PFPA) brush-grafted particles after 10 % treatment with amino-terminated PEG. It allows antibodies more easily approach the polymer brushes, which become swollen slightly in water. This study that demonstrates poly(PFPA) brush-based platforms as the alternative tools for IP

would suggest the capability of those platforms to be applied to a wide variety of bio-applications based on biomolecule immobilization.

Chapter 5. Reactive Polymer-Based Platforms for Biosensing Applications

This works is currently done with the laboratories of Prof. Sheng Li, Yoosik Kim and Sungyun Jeon in KAIST.

5.1. Introduction

Biosensor is an analytical device, used for the detection of an analyte, that combines a biological component with a physicochemical detector such as an electrical signal or fluorescent optical signal.[1-3] The bioreceptor is designed to interact with the specific analyte of interest to produce an effect measurable by the transducer. High selectivity for the analyte among a matrix of other chemical or biological components is a key requirement of the bioreceptor. Common types of bioreceptor interactions involve antibody-antigen[4], enzymes-ligands[5], nucleic acids-DNA[6], cellular structures-cells[7], or biomimetic materials.

Surface attachment of the biological elements is an important part in a biosensor.[8] The simple way to functionalize the surface is the use of aminosilane, polylysine, or epoxy silane on the surface of silicon wafers or glasses.[9] In this study, we added poly(PFPA) after the treatment with aminosilane[10-14], which have quantitative and very reactive functional groups in the chains to allow more biomolecules be grafted on the surface of sensors. The characterization of aminosilane-coated surface and poly(PFPA) films were done by elipsometry and confocal microscopes using fluorescent antibodies. According to further

investigation of the realization of poly(PFPA)-coated channel with proper amount of antibodies for detection[15], these poly(PFPA)-based platforms could be expected to be alternative platforms for the application of in vitro diagnosis sensors.

5.2. Experimental Section

Materials. All chemicals and solvents were purchased from Sigma-Aldrich and used as received. Poly(PFPA) polymers were polymerized as mentioned in chapter 2. Silica gel for column chromatography was purchased from Merck Chemical Company. Silicon wafer (100) and glass were used as substrates to prepare polymer film. Fluorescent antibodies used in this part is Alexa 555, anti-mouse.

Characterization. ^{1}H NMR spectra and ^{19}F NMR spectra were recorded on a Bruker Avance 500 MHz FT-NMR spectrometer. Chemical shifts were given in ppm relative to trimethylsilane (TMS). Gel permeation chromatography (GPC) was used to determine the molecular weight and the corresponding molecular weight distributions (M_w/M_n) of the polymer samples. GPC (YL9100, Young Lin Instrument Co. LTD.) measurements were performed under poly(styrene) standards in THF with 5 mg/mL polymer sample concentration. The film thickness were obtained by a variable-angle multiwavelength ellipsometer (Gaertner L2W15S830, Gaertner Scientific Corp.). For direct antibody visualization, glycerol based mounting solution was applied onto antibody-conjugated silicon wafer, then examined with Zeiss LSM 700 confocal microscope using C-Apochromat 40x lens with NA = 1.2.

Surface Modification with APTES by Silanization. Bare silicon wafers and

glasses were washed 2 times with ethanol and sonicated in ethanol for 5 min. The substrates were dried in nitrogen stream and at 110 ℃ for 30 min. For organic phase deposition, two substrates were placed in vial and sealed with septum, and then purged with nitrogen gas for 5 -10 min. APTES solution in anhydrous toluene in the separate vial was purged with nitrogen gas. 5 ml solution of APTES was added into the vial of substrates and the vial was shaken for 2 hr at room temperature on the rocker. After reaction, substrates were washed with toluene, methanol, and deionized water and dried in vacuum oven overnight at room temperature.

Attachment of Poly(PFPA) on APTES-Coated Films. APTES-modified substrates were dipped in the solution of 5 wt% poly(PFPA) (35 kg/mol) in toluene and shaken in the rocker. Dipped poly(PFPA)-attached substrates were washed with toluene several times and dried in nitrogen stream. In addition, poly(PFPA) films were fabricated by spin-coating method using the solution of 3 wt% poly(PFPA) with a spin-rate of 5000 rpm for 30 s. The polymer-coated films were annealed at 130 ℃ for 1 hr in an oven.

Antibody Incubation. Fluorescent antibodies (Alexa 555, anti-mouse) 6.67 ul in 400 ul PBS solution were placed in 24-well plate. Poly(PFPA)-coated substrates were dipped in the solution for 3 hr with a rocker at 4 ℃. After incubation, the substrates were rinsed three times with PBS.

Fabrication of PDMS Channels and Modification of Surfaces with APTES and Poly(PFPA). 40 g of **s**ylgard 184 silicone elastomer base and 4 g of sylgard 184 elastomer curing agent were mixed in the container. The mixture was poured onto the printed Si substrate with the shape of the channel fixed to the square petri dish. To remove air bubbles, the substrates were placed in a desiccator and vacuum was applied for 30 minutes. After baked in an oven at 80 ℃ for 90 min, the PDMS frame was cut into a suitable shape using a mass, and punch holes between the channels.

PDMS was bonded on the silicon wafer and APTES-coated channels were fabricated by spin-coating method with 10 % APTES solution in toluene. APTES-coated channel was dried at 110 ℃ for 1 hr in the oven. Followed by spin-coating with poly(PFPA) solution, the films were annealed at 130 ℃ for 1 hr in the oven and used for antibody attachment.

5.3. Results and Discussion

5.3.1. Fabrication of Poly(PFPA) Film Based on APTES Coating

In previous studies in chapter 2, we used poly(PFPA) thin films, fabricated by spin-coating method, but they showed dissolution behavior in reaction solutions during post-polymerization modification. For biosensors, antibody immobilization and the surfaces which antibodies are attached stably on are required. To improve the stability of poly(PFPA) film on the substrates, we tried to utilize silanization with 3-aminopropyl triethoxysilane (APTES), which make amine groups on the surface. The modified surfaces were applied to attachment of poly(PFPA) by covalent bonding between primary amine and pentafluorophenyl groups.

For organic phase deposition of APTES, substrates were treated with APTES solution in anhydrous toluene in the sealed vial, purged with nitrogen gas. The vial was shaken for 2 hr at room temperature on the rocker. After the poly(PFPA) treatment, substrates were annealed at high temperature for 1 hr. In the case of poly(PFPA) treatment, two different methods were used. First, APTES-coated substrates were dipped into 5 wt% solution of poly(PFPA), and washed and then immersed in deionized water for 3 hours to test the stability for incubation and shaking in antibody solution. However, thickness changes from 19. 67 nm (MSE=3.18) to 8.25 nm (MSE = 3.45) happens after DI water immersion and no uniform surfaces were shown. Next, we tried to make films by spin-coating method using 3 wt % poly(PFPA) solution with 5000 rpm. Annealed poly(PFPA)-coated films with more uniformed surface were immersed in water and no thickness change occurs (from 71 nm (MSE=13) to 70.87 nm (MSE=13.98)).

For the reactivity of poly(PFPA) to antibodies, the antibodies with fluorescent dye such as Alexa 488 and 555 were treated on the surface of poly(PFPA) films, measured by confocal microscopes. Figure 29 shows the effect of APTES on the stable poly(PFPA)-coating and obviously the signals of antibodies increased when using APTES as pre-treatment. The signal is improved in all parts and thus APTES plays an important role as an anchoring group to hold polymers. Despite the good signals of red fluorescence, there is kind of lattice pattern of coating. In order to find out the factor that affects that, we tried the glycine quenching on poly(PFPA). After glycine saturation of antibody-poly(PFPA)-coated films, different antibodies emitted with green were treated. We assumed that, when green antibodies are attached with the appearance of green signals, it will be an APTES effect. As shown in Figure 30 and 31, both red and green signals were detected. In the case of no glycine quenching, the red and green signals appear together in same area. The green antibody was attached to the polymer functional group which did not react with the red antibody, so that it was confirmed that the signals of most of them overlap each other (Figure 30). In the case of glycine quenching, Figure 31 demonstrates some of PFP groups remained after the treatment with red-fluorescent antibodies and even after the treatment with glycine. Overdose of glycine was thought to be unlikely to detect the green antibody in the sample. So we increased the green signal intensity on the microscope and found that it overlaps with some red parts. In other words, it was confirmed that the green antibody was less attached due to glycine quenching. After increased the signal of green, poly(PFPA) polymer group still exist, so polymer groups that did not react with antibodies with extra red dye can react with the antibody with green dye. Also, through the scratch area, it was found that the

abnormally red portion on the microscope was not a background but an antibody-conjugated polymer. APTES is covalently bonded to the substrate and is not expected to be scratched well.

Furthermore, to achieve the patterned surface like channel, we thought about many processing methods such as the fabrication of channels after polymer coating, or the polymer-coating on the sealed areas in the shape of channels, or inside the prepared channels. For the convenient way, we first tested with the substrates after Teflon tape sealed the half of the area. The wrapped area was expected not to exposed on the poly(PFPA). Figure 32 shows the confocal images of red-fluorescent antibody-poly(PFPA)-coated films on silicon wafers. Teflon wrapped sample before the APTES showed no signs of any dye in the taping part, while sample after the APTES attachment showed the point signal in the taping part. These point signal was seemed to be the bond between APTES and antibody with dye, which means that poly(PFPA) coating have an effect on most signals rather than APTES.

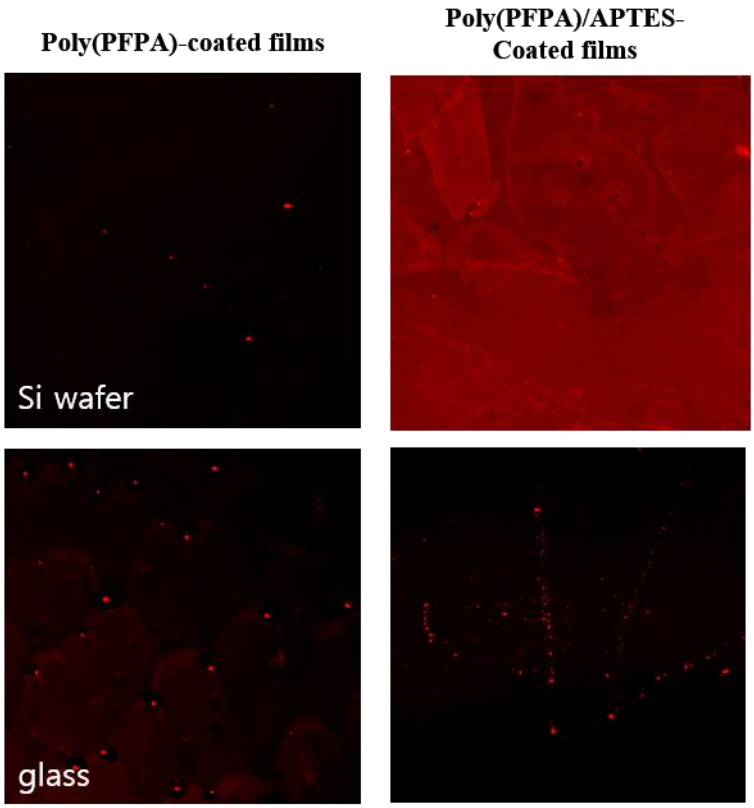

Figure 29 Confocal images of red-fluorescent antibody-poly(PFPA)-coated films on silicon wafers and glasses with (right) and without (left) APTES coating step.

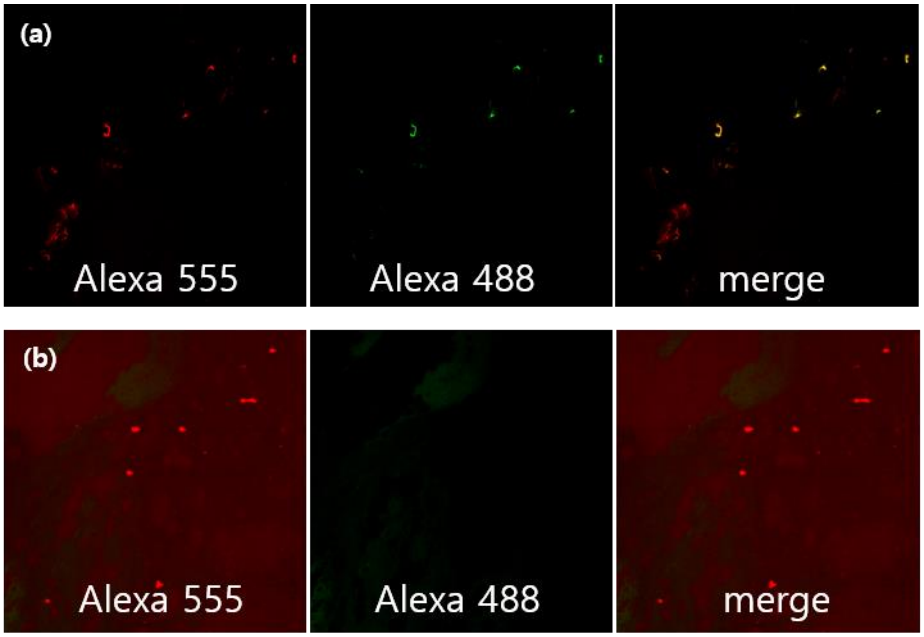

Figure 30 (a) Confocal images of poly(PFPA)-coated films with fluorescent antibodies attached without glycine quenching. Followed by the attachment with red fluorescent antibodies, green fluorescent antibodies were treated, which reacted with remained PFP groups. (b) Images were taken in the different area. The green and red signals of antibodies were overlapped each other.

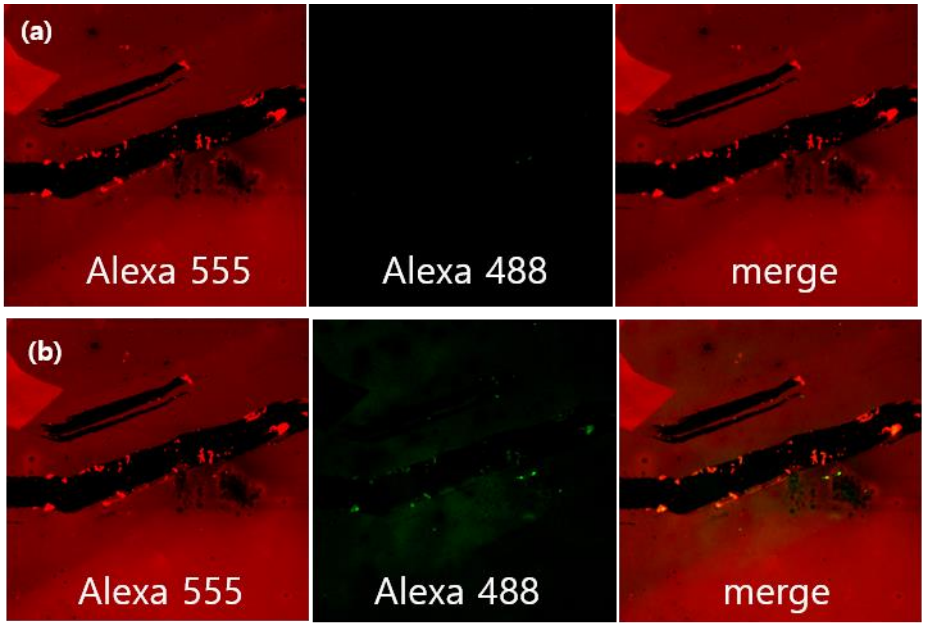

Figure 31 (a) Confocal images of poly(PFPA)-coated films with fluorescent antibodies attached after glycine quenching. Followed by glycine quenching, green fluorescent antibodies were treated, which reacted with remained PFP groups. (b) Images were taken in the same area after the increase of green signal.

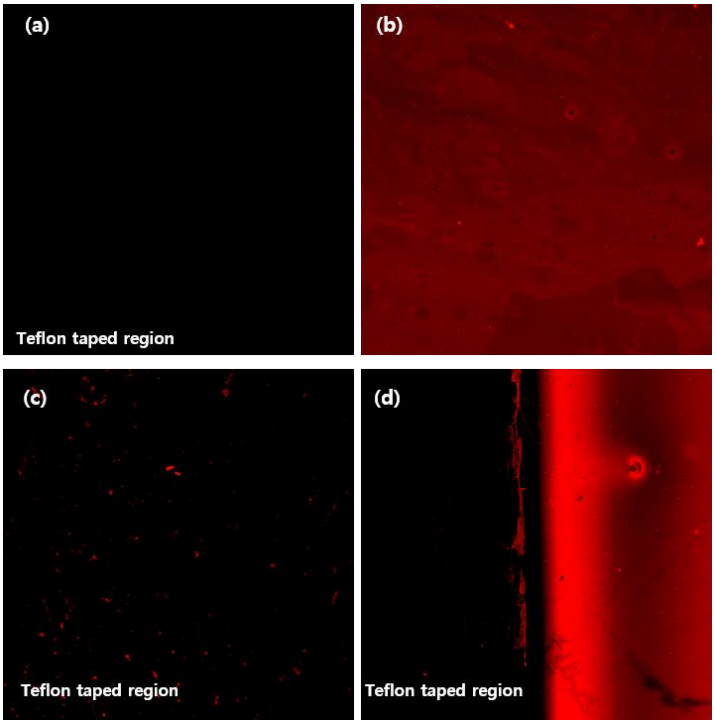

Figure 32 Confocal images of red-fluorescent antibody-poly(PFPA)-coated films on silicon wafers. Teflon taped region before and after treatment of APTES demonstrates the difference, compared with the non-taped region with red fluorescent signals.

5.3.2. Fabrication of Poly(PFPA)-Coated PDMS Channels for Biosensor Application

For the biosensors, the antibodies were placed inside the channel to detect the target antigens. Then poly(PFPA) solution was coated for immobilization of antibodies after the fabrication of channels.

Bonding of PDMS with silicon substrates was good compared to the glass with PDMS. APTES is coated on the bottom surface of the channel and the following coating with poly(PFPA) solution was done. But the air in the clogged portion of the channel thermally expanded after annealing at 110 ℃ so that the bonding between the substrate and the PDMS weakened. Future studies of new design of opened channel would be need. As shown in figure 33, confocal images are taken along the shape of the coated channel. Red signal exists only in the channel, but signal was not great like before samples. (Laser: 2.8%, gain: 818.3; before sample; Laser: 2.2%, gain: 586.0) The hydrophobicity of poly(PFPA) in narrow channel cause dewetting of antibodies during the incubation. Therefore, despite the confirmed reactivity of poly(PFPA) with antibodies and the capability of capturing target antigen as shown in chapter 4, more controlled coating of poly(PFPA) is required for application of biosensors.

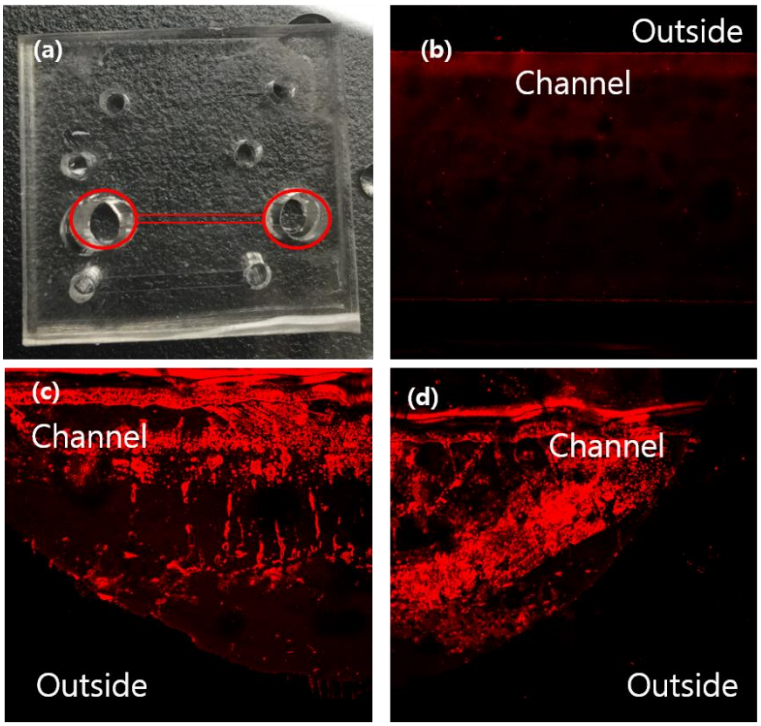

Figure 33 (a) PDMS channels on silicon substrates. (b-d) Confocal images of poly(PFPA)-coated parts after incubation in red fluorescent antibodies. (b) and (c) shows the circular parts and (d) shows the narrow channel part.

5.4. Conclusion

Poly(PFPA)-based platforms have many possibilities to be applied to diverse applications due to its high reactivity with amines. Biomolecules such as antibodies or DNAs could be easily bonded with poly(PFPA) and perform its function as studied in chapter 4. This chapter suggest the poly(PFPA) films based on APTES coating for stability as the new materials for biosensors. Good antibody attachment is achieved by controlled APTES conditions and chemical properties of poly(PFPA). Based on this studies, we believe poly(PFPA)-based films could be expected as alternative method for the facile fabrication of in vitro diagnosis sensors.

References

Chapter 1

1 D. Kessler, F. D. Jochum, J. Choi, K. Char and P. Theato, *ACS Applied Materials & Interfaces* **2011**, *3*, 124-128.

2 W. Zhang and H. Choi, *Polymers* **2014**, *6*, 2803.

3 F. D. Jochum, P. J. Roth, D. Kessler and P. Theato, *Biomacromolecules* **2010**, *11*, 2432-2439.

4 J. L. Zhang, R. S. Srivastava and R. D. K. Misra, *Langmuir* **2007**, *23*, 6342-6351.

5 J.-H. Lee, H. J. Hwang, G. Bhak, Y. Jang, S. R. Paik and K. Char, *ACS Macro Letters* **2013**, *2*, 688-693.

6 L. Ruiz-Pérez, A. Pryke, M. Sommer, G. Battaglia, I. Soutar, L. Swanson and M. Geoghegan, *Macromolecules* **2008**, *41*, 2203-2211.

7 Y. Cho, J. Lim and K. Char, *Soft Matter* **2012**, *8*, 10271-10278.

8 M. A. Nash and H. E. Gaub, *ACS Nano* **2012**, *6*, 10735-10742.

9 S. H. Anastasiadis, M. I. Lygeraki, A. Athanassiou, M. Farsari and D. Pisignano, *Journal of Adhesion Science and Technology* **2008**, *22*, 1853-1868.

10 Q. Zhang, N. Re Ko and J. Kwon Oh, *Chemical Communications* **2012**, *48*,7542-7552.

11 M. Zrínyi, A. Szilágyi, G. Filipcsei, J. Fehér, J. Szalma and G. Móczár, *Polymers for Advanced Technologies* **2001**, *12*, 501-505.

12 H. Lee, S. M. Dellatore, W. M. Miller and P. B. Messersmith, *Science* **2007**, *318*, 426-430.

13 D. Wenzlik, C. Ohm, C. Serra and R. Zentel, *Soft Matter* **2011**, *7*, 2340-2344.

14 H. Yoon, A. Ghosh, J. Y. Han, S. H. Sung, W. B. Lee and K. Char, *Advanced Functional Materials* **2012**, *22*, 3723-3728.

15 A. A. Golriz, T. Kaule, J. Heller, M. B. Untch, P. Schattling, P. Theato, M.

Toda, S. Yoshida, T. Ono, H.-J. Butt, J. S. Gutmann and R. Berger, *Nanoscale* **2011**, *3*, 5049-5058.

16 S. C. Thickett and R. G. Gilbert, *Polymer* **2007**, *48*, 6965-6991.

17 R. K. Iha, K. L. Wooley, A. M. Nyström, D. J. Burke, M. J. Kade and C. J. Hawker, *Chemical Reviews* **2009**, *109*, 5620-5686.

18 C. E. Hoyle and C. N. Bowman, *Angewandte Chemie International Edition* **2010**, *49*, 1540-1573.

19 A. Sanyal, *Macromolecular Chemistry and Physics* **2010**, *211*, 1417-1425.

20 K. Kataoka, A. Harada and Y. Nagasaki, *Advanced Drug Delivery Reviews* **2001**, *47*, 113-131.

21 Y.-P. Sun and H. W. Rollins, *Chemical Physics Letters* **1998**, *288*, 585-588.

22 J. Seo, J. L. Lutkenhaus, J. Kim, P. T. Hammond and K. Char, *Langmuir* **2008**, *24*, 7995-8000.

23 H. S. Suh, H. Kang, P. F. Nealey and K. Char, *Macromolecules* **2010**, *43*, 4744-4751.

24 A. Chilkoti, B. L. Schwartz, R. D. Smith, C. J. Long, P. S. Stayton, *Nature Biotechnology* **1995,** *13*, 1198.

25 H. Takeuchi, J. Thongborisute, Y. Matsui, H. Sugihara, H. Yamamoto, Y. Kawashima, *Advanced Drug Delivery Reviews* **2005,** *57*, (11), 1583-1594.

26 M. Gandhi, R. Srikar, A. L. Yarin, C. M. Megaridis, R. A. Gemeinhart, *Molecular Pharmaceutics* **2009,** *6*, (2), 641-647.

27 J. M. Chan, L. Zhang, R. Tong, D. Ghosh, W. Gao, G. Liao, K. P. Yuet, D. Gray, J.-W. Rhee, J. Cheng, G. Golomb, P. Libby, R. Langer, O. C. Farokhzad, *Proceedings of National Academy of Sciences of the United States of America* **2010,** *107*, (5), 2213-2218.

28 B. Johnsson, S. Löfås, S.; G. Lindquist, *Analytical Biochemistry* **1991,** *198*, (2), 268-277.

29 C. Kurzawa, A. Hengstenberg, W. Schuhmann, *Analytical Chemistry* **2002,** *74*, (2), 355-361.

30 S. Tugulu, A. Arnold, I. Sielaff, K. Johnsson, H.-A. Klok *Biomacromolecules* **2005,** *6*, (3), 1602-1607.

31 C.-C. You, O. R. Miranda, B. Gider, P. S. Ghosh, I.-B. Kim, B. Erdogan, S. A. Krovi, U. H. F. Bunz, V. M. Rotello *Nature Nanotechnology* **2007,** *2*, 318.

32 H. Vaisocherová, W. Yang, Z. Zhang, Z. Cao, G. Cheng, M. Piliarik, J. Homola, S. Jiang *Analytical Chemistry* **2008,** *80*, (20), 7894-7901.

33 J. Trmcic-Cvitas, E. Hasan, M. Ramstedt, X. Li, M. A. Cooper, C. Abell, W. T. S. Huck, J. E. Gautrot *Biomacromolecules* **2009,** *10*, (10), 2885-2894.

34 H. O. Ham, Z. Liu, K. H. A. Lau, H. Lee, P. B. Messersmith *Angewandte Chemie* **2011,** *123*, (3), 758-762.

35 A. T. Nguyen, J. Baggerman, J. M. J. Paulusse, H. Zuilhof, C. J. M. van Rijn, *Langmuir* **2012,** *28*, (1), 604-610.

36 O. I. Kalaoglu-Altan, R. Sanyal, A. Sanyal *Biomacromolecules* **2015,** *16*, (5), 1590-1597.

37 P. Cuatrecasas *The Journal of Biological Chemistry* **1970,** *245*, (12), 3059-3065.

38 M. W. H. Roberts, C. M.Ongkudon, G. M. Forde, M. K. Danquah *Journal of Separation Science* **2009,** *32*, (15-16), 2485-2494.

39 M. E. Sandison, S. A. Cumming, W. Kolch, A. R. Pitt *Lab on a Chip* **2010,** *10*, (20), 2805-2813.

40 S. Avvakumova, M. Colombo, P. Tortora, D. Prosperi *Trends in Biotechnolgy* **2014,** *32*, (1), 11-20.

41 X. Hu, X. Jing, In *A Handbook of Applied Biopolymer Technology: Synthesis, Degradation and Applications*. S. K. Sharma, A. Mudhoo, Eds.; Royal Society of Chemistry: 2011; p 291-310.

42 E. Reimhult, F. Höök, F. *Sensors* **2015,** *15*, (1), 1635-1675.

43 V. Hlady, J. Buijs, H. P. Jennissen *Methods of Enzymology* **1999,** *309*, 402-429.

44 A. Pollak, H. Blumenfeld, M. Wax, R. L. Baughn, G. M. Whitesides *Journal*

of American Chemical Society **1980,** *102*, (20), 6324-6336.

45 Z. Zhang, S. Chen, S. Jiang, *Biomacromolecules* **2006,** *7*, (12), 3311-3315.

46 Y. Yao, Y.-Z. Ma, M. Qin, X.-J. Ma, C. Wang, X.-Z. Feng, *Colloids and Surfaces B: Biointerfaces* **2008,** *66*, (2), 233-239.

47 P. Akkahat, S. Kiatkamjornwong, S.-i. Yusa, V. P. Hoven, Y. Iwasaki, *Langmuir* **2012,** *28*, (13), 5872-5881.

48 J. Ma, S. Luan, L. Song, S. Yuan, S. Yan, J. Jin, J. Yin, *Chemical Communications* **2015**.

49 T. H. Sisson, C. W. Castor, *J. Immunol. Methods* **1990,** *127*, (2), 215-220.

50 S. Niranjanakumari, E. Lasda, R. Brazas, M. A. Garcia-Blanco, *Methods* **2002,** *26*, (2), 182-190.

51 D. Hoenders, T. Tigges, A. Walther, *Polymer Chemistry* **2015,** *6*, (3), 476-486.

52 Kessler, S. W. *Journal of Immunology* **1975,** *115*, (6), 1617-1624.

53 Kessler, S. W. *Journal of Immunology* **1976,** *117*, (5 Part 1), 1482-1490.

54 Blake, M. S.; Johnston, K. H.; Russell-Jones, G. J.; Gotschlich, E. C. A Rapid, *Anal. Biochem.* **1984,** *136*, (1), 175-179.

55 Rusmini, F.; Zhong, Z.; Feijen, J. *Biomacromolecules* **2007,** *8*, (6), 1775-1789.

56 J. Huang, H. Murata, R. R. Koepsel, A. J. Russell and K. Matyjaszewski, *Biomacromolecules* **2007**, *8*, 1396-1399.

57 D. M. Jones, J. R. Smith, W. T. S. Huck and C. Alexander, *Advanced Materials* **2002**, *14*, 1130-1134.

58 H.-U. Blaser, C. Malan, B. Pugin, F. Spindler, H. Steiner and M. Studer, *Advanced Synthesis & Catalysis* **2003**, *345*, 103-151.

59 S. R. Neufeldt and M. S. Sanford, *Accounts of Chemical Research* **2012**, *45*, 936-946.

60 L. R. Domingo, E. Chamorro and P. Pérez, *The Journal of Organic Chemistry* **2008**, *73*, 4615-4624.

61 H. G. Batz, G. Franzmann and H. Ringsdorf, *Die Makromolekulare Chemie* **1973**, *172*, 27-47.
62 P. Ferruti, A. Bettelli and A. Feré, *Polymer* **1972**, *13*, 462-464.
63 P. Theato, *Journal of Polymer Science Part A: Polymer Chemistry* **2008**, *46*, 6677-6687.
64 M. Eberhardt, R. Mruk, R. Zentel and P. Théato, *European Polymer Journal* **2005**, *41*, 1569-1575.
65 J.-C. Blazejewski, J. W. Hofstraat, C. Lequesne, C. Wakselman and U. E. Wiersum, *Journal of Fluorine Chemistry* **1999**, *97*, 191-199.
66 N. Vogel and P. Théato, *Macromolecular Symposia* **2007**, *249-250*, 383-391.
67 M. Eberhardt and P. Théato, *Macromolecular Rapid Communications* **2005**, *26*, 1488-1493.
68 N. Metz and P. Theato, *European Polymer Journal* **2007**, *43*, 1202-1209.

Chapter 2

1 Ulbricht, M. *Polymer* **2006**, **47**, 2217-2262.
2 Deng, X., Eyster, T. W., Elkasabi, Y. & Lahann, J. *Macromolecular Rapid Communications* **2012**, **33**, 640-645.
3 Kessler, D., Jochum, F. D., Choi, J., Char, K. & Theato, P. *ACS Applied Materials & Interfaces* **2011**, **3**, 124-128.
4 Cheng, Q. F., Li, M. Z., Yang, F., Liu, M. J., Li, L., Wang, S. T. & Jiang, L. *Soft Matter* **2012**, **8**, 6740-6743.
5 Duong, H. T. T., Marquis, C. P., Whittaker, M., Davis, T. P. & Boyer, C. *Macromolecules* **2011**, **44**, 8008-8019.
6 Hoenders, D., Tigges, T. & Walther, A. *Polymer Chemistry* **2015**, **6**, 476-486.
7 Arnold, R. M. & Locklin, J. *Langmuir* **2013**, **29**, 5920-5926.
8 Arnold, R. M., McNitt, C. D., Popik, V. V. & Locklin, J. *Chemical Communications* **2014**, **50**, 5307-5309.

9 Zhao, H., Gu, W., Thielke, M. W., Sterner, E., Tsai, T., Russell, T. P., Coughlin, E. B. & Theato, P. *Macromolecules* **2013**, **46**, 5195-5201.

10 Seo, J., Schattling, P., Lang, T., Jochum, F., Nilles, K., Theato, P. & Char, K. *Langmuir* **2010**, **26**, 1830-1836.

11 Son, H., Jang, Y., Koo, J., Lee, J.-S., Theato, P., Char, K. *Polym. J.* **2016**, **48**, 487-495.

12 Jang, Y., Akgun, B., Kim, H., Satija, S. & Char, K. *Macromolecules* **2012**, **45**, 3542-3549.

13 Jang, Y., Seo, J., Akgun, B., Satija, S. & Char, K. *Macromolecules* **2013**, **46**, 4580-4588.

14 Papanu, J. S., Soane, D. S., Bell, A. T. & Hess, D. W. *J Appl Polym Sci* **1989**, **38**, 859-885.

15 Pekcan, Ö., Canpolat, M. & Kaya, D. *J Appl Polym Sci* **1996**, **60**, 2105-2112.

16 Miller-Chou, B. A. & Koenig, J. L. *Prog Polym Sci* **2003**, **28**, 1223-1270.

17 Sivaniah, E., Hayashi, Y., Iino, M., Hashimoto, T. & Fukunaga, K. *Macromolecules* **2003**, **36**, 5894.

18 Eberhardt, M., Mruk, R., Zentel, R. & Théato, P. *European Polymer Journal* **2005**, **41**, 1569-1575.

19 Choi, J., Schattling, P., Jochum, F. D., Pyun, J., Char, K. & Theato, P. *Journal of Polymer Science Part A: Polymer Chemistry* **2012**, **50**, 4010-4018.

20 Sauerbrey, G. *Z Phys* **1959**, **155**, 206-222.

21 Fetters, L. J., Lohse, D. J. & Colby, R. H. in *Physical Properties of Polymers Handbook* (ed Mark, J.) Ch. 25, 447-454 (Springer New York, NY, USA, 2007).

Chapter 3

1 R. Tangirala, E. Baer, A. Hiltner and C. Weder, *Advanced Functional Materials* **2004**, *14*, 595-604.

2 J. Jiang, B. Qi, M. Lepage and Y. Zhao, *Macromolecules* **2007**, *40*, 790-792.

3 N. Ishikawa, M. Furutani and K. Arimitsu, *ACS Macro Letters* **2015**, *4*, 741-744.

4 J. Seo, J. L. Lutkenhaus, J. Kim, P. T. Hammond and K. Char, *Langmuir* **2008**, *24*, 7995-8000.

5 S. Ghorai, J. C. Sumrak, K. M. Hutchins, D.-K. Bucar, A. V. Tivanski and L. R. MacGillivray, *Chemical Science* **2013**, *4*, 4304-4308.

6 J. W. Chung, K. Lee, C. Neikirk, C. M. Nelson and R. D. Priestley, *Small* **2012**, *8*, 1693-1700.

7 F. Jia, Y. Wang, H. Wang, Q. Jin, T. Cai, Y. Chen and J. Ji, *Polymer Chemistry* **2015**, *6*, 2069-2075.

8 Y. Lee, J. Pyun, J. Lim, K. Char, *Journal of Polymer Science Part A: Polymer Chemistry*, **2016**, 54, 1895-1901.

9 A. Balbi, E. Sottofattori, T. Grandi, M. Mazzei, D. S. Pyshnyi, S. G. Lokhov and A. V. Lebedev, *Bioorganic & Medicinal Chemistry* **1997**, *5*, 1903-1910.

10 A. Vacca, C. Nativi, M. Cacciarini, R. Pergoli and S. Roelens, *Journal of the American Chemical Society* **2004**, *126*, 16456-16465.

11 E. J. Foster, E. B. Berda and E. W. Meijer, *Journal of Polymer Science Part A: Polymer Chemistry* **2011**, *49*, 118-126.

12 T. Wolff and H. Gorner, *Physical Chemistry Chemical Physics* **2004**, *6*, 368-376.

13 N. C. Greenham, X. Peng and A. P. Alivisatos, *Physical Review B* **1996**, *54*, 17628-17637.

14 B. S. Lukyanov and M. B. Lukyanova, *Chemistry of HeterocyclicCompounds* **2005**, *41*, 281-311.

15 H. G. Schild, *Progress in Polymer Science* **1992**, *17*, 163-249.

16 M. I. Gibson and R. K. O'Reilly, *Chemical Society Reviews* **2013**, *42*, 7204-7213.

17 S. T. Milner, *Science (Washington, D. C., 1883-)* **1991**, *251*, 905-914.

18 (a) Kessler, D.; Nilles, K.; Theato, P. *J. Mater. Chem.* **2009**, 19, 8184–8189. (b) Roth, P. J.; Theato, P. *Chem. Mater*. **2008**, 20, 1614–1621.

19 Jochum, F. D.; Zur Borg, L.; Roth, P. J.; Theato, P. *Macromolecules* **2009**, 42, 7854–7862.

20 Eberhardt, M.; Mruk, R.; Zentel, R.; Theato, P. *Eur. Polym. J.* **2005**, 41, 1569–1575.

21 Kessler, D.; Roth, P. J.; Theato, P. *Langmuir* **2009**, 25, 10068–10076.

22 Jochum, F. D.; Theato, P. *Macromolecules* **2009**, 42, 5941–5945.

23 Baum, M.; Brittain, W. J. *Macromolecules* **2002**, 35, 610–615.

24 (a) Turgman-Cohen, S.; Genzer, J. *Macromolecules* **2010**, 43, 9567–9577; (b) Turgman-Cohen, S.; Genzer, J. *J. Am. Chem. Soc.* **2011**, 133, 17567–17569.

25 Marko, J. F. *Macromolecules* **1993**, **26**, 313-319.

26 Gallagher, P. D., Satija, S. K., Karim, A., Douglas, J. F. & Fetters, L. J. *Journal of Polymer Science Part B: Polymer Physics* **2004**, **42**, 4126-4131.

27 Seo, J.; Schattling, P.; Lang, T.; Jochum, F.; Nilles, K.; Theato, P.; Char, K. *Langmuir* **2010**, 26, 1830–1836.

28 Benoit, D. N.; Zhu, H.; Lilierose M. H.; Verm, R. A.; Ali, N.; Morrison, A. N.; Fortner, J. D.; Avendano C.; Colvin, V. L. *Anal Chem.* **2012**, 84, 9238-9245.

Chapter 4

1 Matson, R. S. & Little, M. C. *Journal of Chromatography A* **1988**, **458**, 67-77.

2 Sisson, T. H. & Castor, C. W. *Journal of Immunological Methods* **1990**, **127**, 215-220.

3 Huang, B. X. & Kim, H.-Y. *PLoS ONE* **2013**, **8**, e61430.

4 McRae, S., Chen, X., Kratz, K., Samanta, D., Henchey, E., Schneider, S. & Emrick, T. *Biomacromolecules* **2012**, **13**, 2099-2109.

5 Yao, Y., Ma, Y.-Z., Qin, M., Ma, X.-J., Wang, C. & Feng, X.-Z. *Colloids and Surfaces B: Biointerfaces* **2008**, **66**, 233-239.

6 Arnold, R. M., Sheppard, G. R. & Locklin, J. *Macromolecules* **2012**, **45**, 5444-5450.

7 Avvakumova, S., Colombo, M., Tortora, P. & Prosperi, D. *Trends in Biotechnology*, **32**, 11-20

8 Tugulu, S., Arnold, A., Sielaff, I., Johnsson, K. & Klok, H.-A. *Biomacromolecules* **2005**, **6**, 1602-1607.

9 Iwata, R., Satoh, R., Iwasaki, Y. & Akiyoshi, K. *Colloids and Surfaces B: Biointerfaces* **2008**, **62**, 288-298.

10 Jain, P., Baker, G. L. & Bruening, M. L. *Annual Review of Analytical Chemistry* **2009**, **2**, 387-408.

11 Hiraoka, A., Miura, I., Murao, O., Kawahara, N., Tominaga, I. & Hattori, M. *Journal of Neuroscience Methods* **1982**, **5**, 221-226.

12 Huang, J., Han, B., Yue, W. & Yan, H. *Journal of Materials Chemistry* **2007**, **17**, 3812-3818.

13 Lee, D., Balmer, J. A., Schmid, A., Tonnar, J., Armes, S. P. & Titman, J. J. *Langmuir* **2010**, **26**, 15592-15598.

14 Hui, C. M., Pietrasik, J., Schmitt, M., Mahoney, C., Choi, J., Bockstaller, M. R. & Matyjaszewski, K. *Chemistry of Materials* **2013**, **26**, 745-762.

15 Son, H., Ku, J., Kim, Y., Li, S., Char, K. *Biomacromolecules* **2018**, **19**, 951-961.

Chapter 5

1 Turner, Anthony; Wilson, George; Kaube, Isao (1987). Biosensors:Fundamentals and Applications. Oxford, UK: Oxford University

Press. p. 770. ISBN 0198547242.

2 Bănică, Florinel-Gabriel (2012). Chemical Sensors and Biosensors:Fundamentals and Applications. Chichester, UK: John Wiley & Sons. p. 576. ISBN 9781118354230.

3 Cavalcanti A, Shirinzadeh B, Zhang M, Kretly LC (2008). "Nanorobot Hardware Architecture for Medical Defense" (PDF). Sensors. 8 (5): 2932–2958.

4 Marazuela, M. & Moreno-Bondi, M. *Anal Bioanal Chem* **2002**, **372**, 664-682.

5 Crivianu-Gaita, V. & Thompson, M. *Biosensors and Bioelectronics* **2016**, **85**, 32-45.

6 Škrlec, K., Štrukelj, B. & Berlec, A. *Trends in Biotechnology*, **33**, 408-418.

7 Jost, C. & Plückthun, A. *Curr Opin Struct Biol* **2014**, **27**, 102-112.

8 Vo-Dinh, T. & Cullum, B. *Fresenius J Anal Chem* **2000**, **366**, 540-551.

9 Pickup, J. C., Zhi, Z.-L., Khan, F., Saxl, T. & Birch, D. J. S. *Diabetes/Metabolism Research and Reviews* **2008**, **24**, 604-610.

10 Flink, S., van Veggel, F. C. J. M. & Reinhoudt, D. N. *J Phys Org Chem* **2001**, **14**, 407-415.

11 Delanoë-Ayari, H., Al Kurdi, R., Vallade, M., Gulino-Debrac, D. & Riveline, D. *Proc Natl Acad Sci U S A* **2004**, **101**, 2229-2234.

12 Gubala, V., Siegrist, J., Monaghan, R., O'Reilly, B., Gandhiraman, R. P., Daniels, S., Williams, D. E. & Ducrée, J. *Analytica Chimica Acta* **2013**, **760**, 75-82.

13 Yatvin, J., Brooks, K. & Locklin, J. *Angewandte Chemie International Edition* **2015**, **54**, 13370-13373.

14 Brooks, K., Yatvin, J., McNitt, C. D., Reese, R. A., Jung, C., Popik, V. V. & Locklin, J. *Langmuir* **2016**, **32**, 6600-6605.

15 Rusmini, F., Zhong, Z. & Feijen, J. *Biomacromolecules* **2007**, **8**, 1775-1789.

국문 초록

기능성 고분자는 생물공학, 광학, 광전자공학 등 다양한 응용분야에서의 응용이 기대되는 재료로써 형광, 외부 자극 응답성, 생체 적합성 등과 같은 고도화된 기능의 구현에 대한 연구가 주로 이루어져왔다. 연구자들은 도입하고자 하는 분야에 따라 다양한 합성과 제조 방법을 바탕으로 기능성 고분자를 기반으로 한 물리적/화학적 특성 및 여러 형태의 구조를 가지는 플랫폼을 제조하였다. 좀더 고도화된 기능과 구조를 가지는 기능성 고분자에 대한 수요가 증가하면서 반응성 에스테르 고분자와 같이 원하는 형태와 기능으로 쉽게 고분자 플랫폼을 제조할 수 있는 전구체 역할을 하는 고분자들이 주목 받기 시작하였다. 조절 가능한 라디칼 중합 방법을 통해 이러한 반응성 고분자와 그를 사용한 박막 또는 고분자 브러쉬 형태의 플랫폼들이 제시되었으며 간단한 개질을 통하여 바이오 분야에 활용될 수 있는 가능성을 확인하였다. 본 박사학위 논문에서는 활성 에스테르 고분자의 한 종류인 펜타플루오페닐 아크릴레이트 (poly(PFPA)) 고분자를 기반으로 박막과 브러쉬의 형태로 제조한 플랫폼을 구축하고 본 고분자의 아민과의 뛰어난 반응성에 근거하여 바이오 분야의 가장 기본 기술인 생체 분자 고정 기술에 응용하고자 하였다. 기능성 고분자의 종류 및 제조 방법과 생체분자 고정 기술의 중요성 및 활성 에스테르 고분자는 1장에서 간략하게 소개하였다.

2장에서는 고분자의 분자량과 아민의 크기라는 두 가지 제어 요인을 조절하여 poly(PFPA) 고분자를 이용하여 스핀코팅 방법으로 제조한 반응성 고분자 박막의 개질을 제어하였다. RAFT 중합으로 합성된, 두 가지 분자량의 poly(PFPA) 스핀코팅 박막은 서로 다른 탄소

사슬 길이를 갖는 일차 알킬 아민에 의해 처리되었을 때 명백한 차이를 나타냈다. 원자간력 현미경과 광학 현미경을 병행하여 박막의 표면 모폴로지 변화를 확인하였을 뿐만 아니라 수정진동자 미세저울을 통하여 아민 치환 키네틱스와 poly(PFPA) 박막으로의 아민의 침투 깊이를 실시간으로 측정하였다. 아민으로 개질된 박막 내부 구조의 변화는 중성자 반사율 장치를 이용하여 분석하였다. 본 연구를 토대로, 일차 알킬 아민의 탄소 사슬 길이와 poly(PFPA)의 분자량 모두 아민의 침투 깊이와 박막 표면에서부터 고분자가 녹아 나가는 현상에 영향을 준다는 것을 확인했다.

3장에서는 표면 개시 라프트 (RAFT) 중합을 통해 poly(PFPA) 고분자를 브러쉬의 형태로 실리카 입자 표면에 중합하고, 분석 기기 등을 활용해 표면개시제의 결합 및 다양한 분자량으로의 중합을 확인하였다. 고분자 브러쉬는 고분자 사슬의 한 쪽 끝이 표면에 고정되어 있어 화학적으로 안정하다는 장점을 가지고 있는 플랫폼이다. 구현된 반응성 고분자 브러쉬 플랫폼은 간단한 개질 과정만으로도 형광 특성을 지니게 됨을 확인했다.

4장에서는 앞서 중합한 poly(PFPA) 브러쉬 플랫폼을 항원-항체 침전법 또는 면역침강법(IP)이라는 바이오 분야에서 자주 사용되는 타겟 단백질 분리 및 측정 기술에 적용 및 기존 방법을 단점을 개선하고자 하였다. 기존에 상용화되어 사용되는 아가로즈 서포트 기반의 방법은 생체 친화적 결합에 의한 좋은 항체 결합 능력을 보이지만 높은 비특이적 결합 및 항체 분리가능성으로 인해 타겟 단백질을 분리하는 과정에서 데이터의 백그라운드가 높아지기 쉽다는 단점을 가지고 있다. 3장에서 제시한 플랫폼은 고분자 브러쉬의 형태로 실리카 입자 표면에 결합되어 있으며 동시에 아민과의 반응성에 의해 항체와 쉽게 다량

으로 결합할 수 있다. Poly(PFPA) 고분자의 소수성 완화를 위한 폴리에틸렌글라이콜(PEG)과의 개질에 이어 항체를 결합시키고 면역침강 실험 결과 기존 방식의 단점이 완전히 개선되었으며, 고분자 브러쉬의 분자량과 PEG 치환 정도를 조절하여 분리 효율 또한 기존 방식과 비슷한 정도로 좋게 나타남을 확인하였다. 이러한 간편함과 다양성은 poly(PFPA) 플랫폼을 새로운 대안으로 생각할 수 있게 하였다.

5장에서는 poly(PFPA)를 코팅한 채널을 제조하여 일차적인 질병 진단센서로의 활용 가능성을 보았다. 표면에 아민 작용기를 가지고 있도록 처리된 기판에 PFPA 고분자를 아민과의 반응을 통해 결합시킨 후 반응하지 않고 남은 고분자의 작용기는 질병 진단을 위한 항체의 결합에 사용되었다. 형광을 띠는 항체를 사용하여 poly(PFPA) 박막의 항체와의 결합 및 안정성, 채널 형태로 제조 가능성 등을 형광 이미지 등을 통해 확인하였다. 4장 및 기존 연구를 통해 확인한 poly(PFPA)의 항체 결합력 및 고정된 항체의 항원 탐지 능력을 기반으로 추가적인 심화 연구를 통하여 일차적인 진단에 사용되는 바이오센서로 활용할 수 있다는 가능성을 제시하였다.

이러한 일련의 연구 결과들을 바탕으로 아민 반응성 poly(PFPA)의 고분자 박막부터 고분자 브러쉬 형태로의 합성 및 간단한 개질 방법에 대한 기초 연구를 통해 제조된 플랫폼이 항체와 같은 생체 분자 고정을 이용한 바이오 분야로의 응용 가능함을 시사하였다.

주요어: 펜타플루오로페닐 아크릴레이트 고분자, 개질, 항체 고정, 면역침강법, 고분자 브러쉬, 표면 개시 라프트 중합

학 번: 2014-30262 **성 명:** 손 현 주